

Reheating after relaxation of large cosmological constant

Paul Martens,¹ Shinji Mukohyama,^{1,2} and Ryo Namba³

¹*Center for Gravitational Physics and Quantum Information,*

Yukawa Institute for Theoretical Physics,

Kyoto University, 606-8502, Kyoto, Japan

²*Kavli Institute for the Physics and Mathematics of the Universe (WPI),*

The University of Tokyo, Kashiwa, Chiba 277-8583, Japan

³*RIKEN Interdisciplinary Theoretical and Mathematical Sciences (iTHEMS), Wako, Saitama 351-0198, Japan*

(Dated: 25th May 2022)

We present a cosmological model of an early-time scenario that incorporates a relaxation process of the would-be large vacuum energy, followed by a reheating era connecting to the standard hot big bang universe. Avoiding fine-tuning the cosmological constant is achieved by the dynamics of a scalar field whose kinetic term is modulated by an inverse power of spacetime curvature [1, 2]. While it is at work against radiative corrections to the dark energy, this mechanism alone would wipe out not only the vacuum energy but also all other matter contents. Our present work aims to complete the scenario by exploiting a null-energy-condition violating sector whose energy is eventually transferred to a reheating sector. We provide an explicit example of this process and thus a concrete scenario of the cosmic onset that realizes the thermal history of the Universe with a negligible cosmological constant.

I. INTRODUCTION

Observational developments in the past few decades have proven their potential to pin down cosmological parameters to high precision. Despite some recent discrepancy in the determination of the observed value of the expansion rate [3–7], it is now a well accepted fact that our Universe as a whole not only expands but at an accelerated rate. What causes the accelerated expansion is often dubbed *dark energy*, though there is no agreed consensus about its true nature. The simplest possibility is the cosmological constant (c.c.); it can be freely added to the Einstein equation with an arbitrary value at the classical level, while quantum-mechanically the zero-point energy possessed by vacuum fluctuations could contribute to it.

The discrepancy between the observed and theoretically expected values of the c.c. is the major source of the so-called c.c. problem. In the viewpoint of quantum field theory, one would sum all zero-point diagrams and thus obtain some value that is subject to UV physics, which should compose the vacuum energy. On the other hand, one might wish that the c.c., written as Λ , which enters in

the Einstein equations, would incorporate all the above contributions. However, if it does then the observational bounds on the c.c. require an enormous cancellation among different contributions. Without such a cancellation, these two numbers would not match, but more than that, they would differ by many orders of magnitude (the observational bounds being extremely smaller) [8–10]. The c.c. problem can thus also be seen as a bridging problem between the cosmological and the quantum worlds, and any significant progress on its resolution could eventually lead to a fundamental progress in both paradigms.

Furthermore, the c.c. problem, while already an issue on its own, begs yet another problem: the *coincidence problem*. It basically asks the following question: why is the small value of the vacuum energy, *i.e.* the density of dark energy, of the same order as that of dark matter today? The scaling of the dark energy density with respect to time is different from that of the dark matter, and only a few Hubble times would deviate their values by orders of magnitude. This implies that we live at a very special moment, nested at the hinge between a dark matter dominated and a dark energy dominated era. Such a coincidence requires a delicate fine tuning [11], leaving us with a speculation that there may be a physical mechanism to realize it.

While numerous attempts have been made to solve the issue, including from supersymmetry perspectives to effective modifications of gravity (see *e.g.* [8, 10] for review and references therein), none have yet provided a satisfactory and definitive answer. One may also be tempted to invoke the so-called *anthropic principle* to give a reasoning to it, *i.e.* the dark energy is so small and the transition occurs now, because the physical conditions to our existence are only reunited at this precise moment and with that physical parameter. While it might as well serve as a valid answer, and one cannot totally refute its relevance, its nature makes it difficult to test and to quantify new predictions out of it. In other words, taking it as the final answer too hastily runs into the risk of missing some more fundamental physical connection, and it therefore appears essential to further investigate a concrete mechanism to address the issue at hand.

Many different paths have been investigated to solve the c.c. problem, and this is not the first time some c.c. relaxation processes, as in our present study, have been considered. For example, one could consider to have the relaxation unfolds during an unconventional inflationary phase [12], to work within the framework of some bouncing Universe scenario by dynamically decreasing the value of c.c. during a contracting phase [13], or to forbid a non-vanishing 4d curvature of a maximally symmetric 3-brane world-volume embedded in 5d spacetime [14, 15]). Ideally, one's solution should eventually be linked to some observational signatures (*e.g.* [16]). While our approach, which is elaborated below, does not yet expose itself to this last test and rather provides a proof of concept

at this stage, it remains within the realm of effective field theories and should still be adaptable for further considerations.

Refs. [1, 2] proposed a model that dynamically relaxes the value of the c.c. to a tiny one thanks to a scalar field that ever rolls down its potential ¹. The kinetic term of this field is modulated by a negative power of the Ricci scalar, and its apparent divergence in the limit of vanishing curvature is dynamically prohibited by the classical motion of the scalar background. The relaxation mechanism operates as the potential of the scalar field dominates over the kinetic term in the same limit, and yet the dynamics results in a vanishing potential, which is the future attractor of the system. Importantly, the potential can include not only that of the scalar itself but also all the other (constant) energy contents, that is,

$$V_{\text{total}} = V_{\text{scalar alone}} + V_{\text{c.c.}} + V_{\text{zero point}} + V_{\text{all others}} , \quad (1)$$

and what approaches to zero is V_{total} ; in a way, the scalar field dynamically fixes its potential value $V_{\text{scalar alone}}$ only to cancel the c.c., the zero point energy and all the other (constant) contributions. Therefore even if large bare cosmological constant and radiative zero point energy were present, the effective vacuum energy would go as $\Lambda_{\text{eff}} \approx V_{\text{total}}/M_{\text{Pl}}^2 \rightarrow 0$ after a long time, and the spacetime geometry would anyway approach a flat one.

This relaxation mechanism partially holds a spirit similar to what Weinberg called ‘adjustment mechanism’ in [8]. The related no-go theorem [8, 10, 17] is evaded in the current mechanism thanks to the fact that, while the theorem only considers the physics at a dynamical equilibrium and thus assumes translational invariance, an essential ingredient of the mechanism considered here is the non-vanishing canonical momentum of the scalar field, rendering the mechanism considered here an exceptional case to the theorem.

However, while this process alone is a powerful mechanism to resolve the c.c. problem, it also effectively empties the Universe as an inevitable consequence, by eventually diluting everything away: the total energy in the Universe — which includes any radiative corrections — is constrained to asymptotically converge to a null value. To connect this empty space to our present Universe, the main purpose of this work is to implement a reheating phase after the c.c. relaxation so that the standard hot big bang scenario is revived. To this aim, we not only construct a stable model that achieves the scenario, but also demonstrate it by exhibiting a concrete realisation along a numerical verification.

¹ This scalar field corresponds to φ_1 in later sections, where the subscript number is introduced to distinguish among three scalar fields that are responsible for different processes in our scenario.

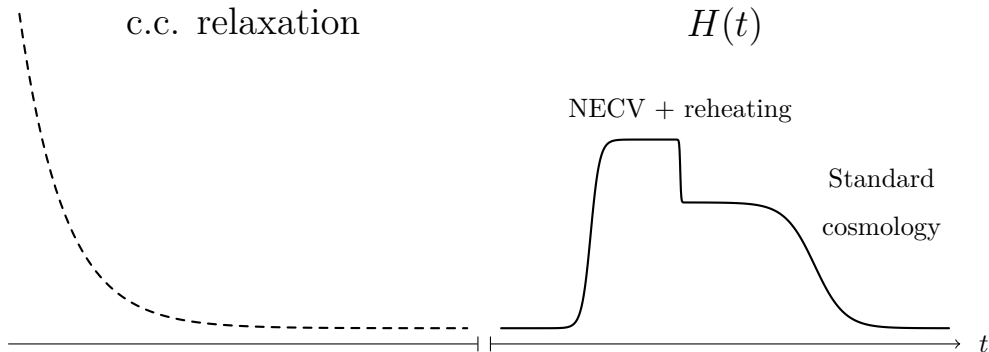


Figure 1. Schematic illustration of the cosmic evolution according to the scenario studied in this paper. The dashed curve on the left corresponds to the initial phase of the c.c. relaxation, and the solid curve on the right depicts the NEC violation and the reheating dynamics. The Universe is eventually filled with radiation and recovers the standard cosmic history. This figure is highly schematic and not to scale.

For the reheating phase, we rely in part on the Lagrangian of the Horndeski theory [18–20], as using the latter has been shown to allow to violate the null energy condition (NEC) in a stable manner [21, 22]. The gravitating energy elevated by the NEC violation is then transferred to another sector that eventually reheats the Universe. In order not to disrupt the c.c. relaxation mechanism, which is always in action, the NEC-violating and reheating phases must occur for sufficiently short time compared to the time scale of the relaxation. Moreover, we assume that these phases take place periodically, and our observed Universe can be the result from any one of those recurring occurrences. *In fine*, the dynamical cosmological constant relaxation described by our model would thus allow us to avoid invoking the anthropic principle to solve the c.c. problem.

To present our model, this work shall first describe the overall cosmic history our model suggests and take this occasion to review the cosmological relaxation process we employ (section II). The NEC-violating and the reheating sectors are then assessed from a theoretical perspective by considering their linear perturbations, explicitly providing the conditions under which we avoid having any ghost or gradient instability against the background dynamics of the desired behavior (section III). We shall then focus on the reheating process, and the model and all its composing functions are now either explicitly chosen or deduced (section IV). Lastly, we use a numerical approach to explicitly and qualitatively witness the whole reheating process unfold (section V), before concluding our study (section VI).

II. OVERALL PICTURE OF THE COSMIC HISTORY

The vacuum energy that drives the accelerated cosmic expansion at the present time is, whatever its true nature is, observed to have an extremely small value, and this smallness demands an explanation. We explore a dynamical solution to this issue, and in this regard, we employ the mechanism originally proposed in [1, 2]. However this mechanism alone leads to an empty universe, that is, it not only reduces the contribution from the c.c. but also dilutes all other contents of the Universe. In order to incorporate an additional process to eventually populate the Universe with energetic radiation, a couple of potential candidates have been sketched in [23]. Our mechanism in this paper shares some aspects with their ‘fast violation’ section but extends it. We later provide a concrete realization of the reheating and show with numerical analyses that the scenario can indeed be achieved without any instability.

To this end, the mechanism we propose to incorporate three essential phases through the cosmic history, namely, in order:

1. **Cosmological constant relaxation.** A large value of the c.c., together with all the other matter content, is dynamically relaxed to the small present value [section II A for summary and [1, 2] for details].
2. **Null energy condition violation.** The Universe is energetically revived by accommodating a phase violating the NEC [section II B for summary and section IV for details].
3. **Reheating.** The Universe reheats and connects this process to the standard cosmological picture [section II B for summary and section IV for details].

This overall picture is schematically illustrated in fig. 1. After the relaxation, the NEC violation re-energize the Universe, which is the first rise of H in the figure; after some time, H quickly drops to some non-zero value, corresponding to the end of the NEC-violating phase during which a fraction of energy is transferred to the reheating sector. Eventually this sector decays to radiation, recovering the standard big bang cosmic history. We assume that the potential for the NEC-violating sector is periodic so that the sequence described above (the c.c. relaxation, NEC violation and reheating) repeats many times until the c.c. actually goes down to the observed tiny value.

The model setup can thus be described by the action

$$S = \int d^4x \sqrt{-g} \left(\mathcal{L}_{\text{E.H.}}[g] + \mathcal{L}_{\text{c.c. relax}}[\varphi_1, g] + \mathcal{L}_{\text{NECV+reh}}[\varphi_2, \varphi_3, g] \right), \quad (2)$$

where $\mathcal{L}_{\text{E.H.}}$, $\mathcal{L}_{\text{c.c. relax}}$ and $\mathcal{L}_{\text{NECV+reh}}$ describe the Einstein-Hilbert part, the c.c. relaxation mechanism, and the combined sector of NEC violation and reheating, respectively. The fields φ_1 , φ_2 and φ_3 are responsible for the c.c. relaxation, NEC violation and reheating, respectively, and g denotes the spacetime metric. Let us note that, as we see below and concretely show in section IV, the reheating sector is nontrivially coupled to the NEC-violating sector, and thus they are not separable at the level of Lagrangian. In the following subsections, we summarize the gist of the c.c. relaxation, NEC violation and reheating sectors individually and the requirements to achieve the desired history of the Universe.

A. Cosmological constant relaxation

We follow [1, 2] to drive an initially large c.c. to the tiny value observed today, and this subsection serves as a brief review of the mechanism. This relaxation mechanism is driven by a scalar field φ_1 that is non-minimally coupled to gravity, and the corresponding Lagrangian $\mathcal{L}_{\text{c.c. relax}}$ together with the Einstein-Hilbert part $\mathcal{L}_{\text{E.H.}}$ introduced in eq. (2) reads

$$\mathcal{L} = \underbrace{\frac{M_{\text{Pl}}^2}{2}R}_{\mathcal{L}_{\text{E.H.}}} + \underbrace{\alpha R^2 + \frac{X_1}{f(R)} - V_1(\varphi_1)}_{\mathcal{L}_{\text{c.c. relax}}}, \quad (3)$$

where we hereafter denote the kinetic terms of scalar fields φ_i ($i = 1, 2, 3$) by

$$X_i \equiv -\frac{1}{2}g^{\mu\nu}\partial_\mu\varphi_i\partial_\nu\varphi_i, \quad (4)$$

and where R is the Ricci scalar of the spacetime metric $g_{\mu\nu}$, V_1 the potential of φ_1 , and M_{Pl} and α are the (normalized) reduced Planck mass and a dimensionless constant, respectively. The curvature quadratic term αR^2 with *e.g.* $\alpha = \mathcal{O}(1)$ (> 0) is needed to tame the instability that would otherwise arise during the course of relaxation. The term is purely gravitational and thus could in principle be combined with the Einstein-Hilbert term $\mathcal{L}_{\text{E.H.}}$ to together compose a gravitational action. Nevertheless, since it only affects the stability during the relaxation and becomes negligible at later stages of our scenario, we simply include it in $\mathcal{L}_{\text{c.c. relax}}$.² Note that any non-zero c.c. term,

² Other higher-order terms of curvature invariants such as $R_{\mu\nu}R^{\mu\nu}$ and $R_{\mu\nu\rho\sigma}R^{\mu\nu\rho\sigma}$ should arise due to quantum corrections. We can always rearrange a linear combination of R^2 , $R_{\mu\nu}R^{\mu\nu}$ and $R_{\mu\nu\rho\sigma}R^{\mu\nu\rho\sigma}$ into another one of R^2 , the Gauss-Bonnet term and the Weyl tensor squared. Since the Gauss-Bonnet term does not contribute to equations of motion, and the Weyl squared term is responsible for the ghost modes in UV, we call the coefficient of R^2 in this linear combination as α appearing in eq. (3). Unless fine-tuned, the coefficients of those higher curvature terms are expected to be of $\mathcal{O}(1)$ in the units of M_{Pl} , and the would-be ghost modes associated with them have masses of order M_{Pl} . Therefore the higher-order terms are irrelevant at energies and momenta sufficiently below the Planck scale, with which we are concerned, and the stability only requires $\alpha > 0$ in IR.

including the vacuum energy originated from the quantum fluctuations of matter fields, can be absorbed into $V_1(\varphi_1)$ without loss of generality.

A crucial part for the mechanism to work is that the coefficient of the kinetic term of φ_1 diverges in the limit of vanishing R . To this end, we demand that f vanishes at $R = 0$ as

$$f(R) \approx \left(\frac{R^2}{M_{\text{Pl}}^4} \right)^m, \quad (5)$$

where m is some positive number and we assume $m > 3/2$ for the reason that we explain later in this subsection. The constant M_{Pl}^4 is introduced to make the function dimensionless, and the overall normalization of f can always be absorbed by redefining X_1 . Since the kinetic term depends nonlinearly on the curvature, the system described by the Lagrangian (3) contains two scalar degrees of freedom. It is straightforward to show that both scalar degrees satisfy the no-ghost condition and that the two speeds of propagation are both unity in the low-energy regime³.

Starting with the kinetic Lagrangian of the assumed form $X_1/f(R)$, quantum corrections may generate a more general kinetic Lagrangian consisting of terms of the form $X_1^{q_i}/(R^2/M_{\text{Pl}}^4)^{m_i}$ ($i = 1, 2, \dots$). In this case, what controls the c.c. relaxation is the most singular-looking term. Fortunately, the more singular-looking the dominant term is, the more robust the c.c. relaxation mechanism is. Therefore, less singular-looking terms generated by quantum corrections do not spoil the c.c. relaxation mechanism, while more singular-looking terms generated by quantum correction simply strengthen it. See [2] for some details. In the rest of the present paper, for simplicity we consider the simplest kinetic Lagrangian consisting of a term with $q_i = 1$ and $m_i = m > 3/2$.

Another important ingredient is that the potential $V_1(\varphi_1)$ crosses zero at some finite value of φ_1 . Starting the evolution from a positive value of V_1 , φ_1 rolls down the potential and approaches 0, around which V_1 can be well approximated by a linear form

$$V_1(\varphi_1) \simeq cM_{\text{Pl}}^3(\varphi_1 - v), \quad (6)$$

where v is the value of φ_1 at which the potential would cross 0 and c is some dimensionless constant. Then, on the flat Friedmann-Lemaître-Robertson-Walker (FLRW) background, the equation of motion for the homogeneous background of φ_1 , denoted by $\bar{\varphi}_1$, takes the form

$$\frac{\partial \Pi_1}{\partial \mathcal{N}} + (3 + \epsilon) \Pi_1 + c = 0, \quad (7)$$

where H is the Hubble expansion rate, $\mathcal{N} \equiv \ln a$ is the number of e-folds with a being the scale factor, $\Pi_1 \equiv H^2 \partial_{\mathcal{N}} \bar{\varphi}_1 / (M_{\text{Pl}}^3 f)$, and $\epsilon \equiv -\partial_{\mathcal{N}} H / H$. Eq. (7) makes it evident that, for a negligible time variation of ϵ , the stationary solution is given by $\Pi_1 \simeq -c(3 + \epsilon)^{-1}$.

³ See *e.g.* section V.A.4 of [24].

At late time the Friedmann equation around the stationary solution takes the approximate form, that is,

$$V_1 \simeq 3M_{\text{Pl}}^2 H^2 . \quad (8)$$

This equation, together with the aforementioned result, leads to the time variation of V_1 as

$$\frac{\partial}{\partial \mathcal{N}} \left(\frac{2V_1}{M_{\text{Pl}}^4} \right)^{2-2m} \simeq 24 c^2 (m-1) \frac{(2-\epsilon)^{2m}}{3+\epsilon} \simeq 2^{2m+3} c^2 (m-1) , \quad (9)$$

where in the last equality the fact that ϵ is small during the relaxation phase is used. This clearly shows that, when V_1 approaches to 0, the field $\bar{\varphi}_1$ in fact stalls, and V_1 never crosses 0, namely

$$V_1 \rightarrow +0 \quad \text{as} \quad \mathcal{N} \rightarrow +\infty \quad (10)$$

is the asymptotic behavior, provided that $m > 3/2$ as we have assumed. In fact, the behavior (10) only requires $m > 1$ besides the smallness of ϵ . However, if the scalar kinetic term X_1/f in eq. (3) dominated over the αR^2 term at low energy ($H \ll M_{\text{Pl}}$), the dynamics of the system would destabilize the stationary solution above [2]. To prevent this, we demand $X_1/f < \alpha R^2$ at low energy, which can be achieved for $m > 3/2$ and is self-consistent with the solution obtained above.

The essence of the mechanism to relax a large c.c. is as described above. It is worth stressing that the most important ingredient is the coefficient of X_1 in eq. (3) that has a singular-looking form in the limit $R \rightarrow 0$, and this mechanism is effective as long as the most singular term among many other possible ones has the behavior described here. While quantum corrections should produce additional regular operators in the action, the motion of $\bar{\varphi}_1$ nonetheless drives the total potential to the vanishing value. On the other hand, one can show that quantum corrections do not generate a potential that is singular at $R = 0$. Singular-looking kinetic terms of the form $X_1^{q_i}/(R/M_{\text{Pl}}^2)^{2m_i}$ ($i = 1, 2, \dots$) can be generated by quantum correction but this does not cause a problem. Actually, the more singular-looking the radiatively-corrected kinetic term is, the more robust the c.c. relaxation mechanism becomes.

Now, we have achieved a tiny value of the c.c./vacuum energy after a sufficiently long time. However, by that same achievement, since, under the condition $m > 3/2$, the potential V_1 approaches zero more slowly than matter and radiation, the Universe would be empty after the mechanism under consideration takes place. The Universe thus needs to be ‘reheated’ once the c.c. is driven to a small value. This is the subject of the subsequent subsections, and is the main purpose of our present study.

B. Null energy condition violation and reheating

After the mechanism in section II A operates, not only the c.c. and vacuum energy but also all other energy contents decrease to a negligible value. In order to connect to the known cosmic thermal history, ‘reheating’ thus needs to subsequently take place to re-populate the Universe with energetic radiation. The NEC is necessarily violated to achieve this scenario, in order for the energy required for reheating to be temporarily available. Another field that mediates the reheating process is destabilised through its coupling to the NEC-violating sector, and its acquired energy is finally transferred to radiation.

In order to stably violate the NEC we employ a subclass of the Horndeski theory [18–20], whose scalar field is now denoted by φ_2 . The reheating field φ_3 couples to this sector, and we introduce direct couplings besides the gravitational one for efficient energy transfer. A minimal setup that satisfies these requirements adopts the following form of the Lagrangian in eq. (2),

$$\mathcal{L}_{\text{NECV+reh}} = K(\varphi_2, X_2, \varphi_3) - G_3(\varphi_2, X_2, \varphi_3) \square \varphi_2 + P(\varphi_3, X_3), \quad (11)$$

where φ_2 invokes the NEC violation. Here K and G_3 are some functions of φ_2 , X_2 and φ_3 , while P is a function of φ_3 and X_3 only. The reheating field φ_3 is implicitly coupled to radiation. For simplicity we assume that $\mathcal{L}_{\text{NECV+reh}}$ is in the Einstein frame and hence the total Lagrangian that is relevant to the present mechanism is $\mathcal{L}_{\text{E.H.}} + \mathcal{L}_{\text{NECV+reh}}$. As far as φ_1 stays almost constant, this assumption is expected to be valid since, as explicitly shown in [2] for linear perturbations, the model (3) recovers general relativity at low energy. For the consistency of this treatment, we shall later clarify what we precisely mean by being ‘almost constant’ and obtain the condition under which φ_1 stays almost constant during the NEC violation and reheating.

The c.c. relaxation sector discussed in section II A is decoupled from the rest of the physics except through gravity. The relaxation mechanism continues to operate throughout the cosmic history to keep the vacuum energy from overdominating the Universe. Since it takes many (current) Hubble times to make the c.c. small enough, we assume that the functions K and G_3 are periodic in the NEC-violating field φ_2 so that a NEC-violating phase occurs periodically and (partial) reheating may occur several times, in order to avoid a miraculous fine-tuning with respect to the timing of reheating. On top of the periodicity, we assume that the functions of φ_2 enjoy approximate shift symmetry for most of its domain and that the NEC violation (and reheating) is restricted to a short duration where the approximate shift symmetry is broken.

For the purpose of presentation, let us for the moment turn off the reheating sector φ_3 in order

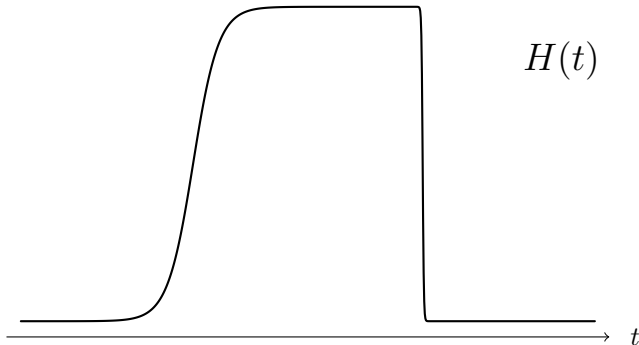


Figure 2. Schematic illustration for the Hubble history, with H the Hubble expansion rate. This figure is simplified in that it only extracts the behavior of the target NEC violation, with all the other sectors, including the c.c. relaxation and reheating sector, turned off.

to focus on the NEC violation part. The Lagrangian of eq. (11) is then reduced to

$$\mathcal{L}_{\text{NECV}} \equiv \mathcal{L}_{\text{NECV+reheat}}|_{\varphi_3=0, P=0} = \tilde{K}(\varphi_2, X_2) - \tilde{G}_3(\varphi_2, X_2) \square \varphi_2, \quad (12)$$

where $\tilde{K} \equiv K|_{\varphi_3=0}$ and $\tilde{G}_3 \equiv G_3|_{\varphi_3=0}$. For simplicity we adopt the following ansatz for \tilde{K} and \tilde{G}_3 , keeping only terms lower-order in X_2 ,

$$\tilde{K} = \tilde{f}_1(\varphi_2) X_2 + \tilde{f}_2(\varphi_2) X_2^2 - \tilde{V}(\varphi_2), \quad \tilde{G}_3 = \tilde{f}(\varphi_2) X_2. \quad (13)$$

The functions \tilde{f}_1 , \tilde{f}_2 and \tilde{f} are periodic in φ_1 with a common period and should have appropriate forms – their respective forms we consider in the present study, especially for the purpose of numerical evaluations, are fixed according to the desired evolution of the Hubble expansion rate H and are reconstructed using the equations of motion. This procedure is discussed in detail in section IV A. With these potential and kinetic structures, the motion of φ_2 accomplishes to violate the NEC and increases the value of H for some finite time. A schematic shape of the resultant evolution of H with the NEC violation is illustrated as a function of time in fig. 2. In this figure, all the matter contents other than the NEC-violating φ_2 are excluded. Once the reheating sector φ_3 couples to φ_2 , the behavior of H is modified to the one captured in fig. 1.

In order to reheat the Universe, the reheating field φ_3 transfers the energy acquired during the NEC-violating period to radiation. It thus couples to φ_2 , and this is realized by reintroducing the φ_3 dependence into the previous functions. Formally, we make the changes

$$\tilde{f}_{1,2}(\varphi_2) \rightarrow f_{1,2}(\varphi_2, \varphi_3), \quad \tilde{f}(\varphi_2) \rightarrow f(\varphi_2, \varphi_3), \quad \tilde{V}(\varphi_2) \rightarrow V(\varphi_2, \varphi_3), \quad (14)$$

and reintroduce $P(\varphi_3, X_3)$. For simplicity we assume that φ_3 is a canonically normalized scalar with a simple potential, except for its coupling to φ_2 via (14). In other words, P , in eq. (11), takes

the form

$$P(\varphi_3, X_3) = X_3 - U(\varphi_3) . \quad (15)$$

Thanks to these couplings in (14), the effective potential of φ_3 basically changes over time with respect to the motion of φ_2 . As already invoked, we assume that φ_2 enjoys approximate shift symmetry for most of its domain except for the short NEC violating period. This in particular means that the effective potential for φ_3 changes only in the vicinity of the NEC violating period. We choose the coupling between φ_2 and φ_3 so that, once the NEC violation starts operating, the effective potential forms a new local minimum in which φ_3 gets trapped. After the NEC-violating phase ends, φ_3 stays at a new minimum for a while, but, after a finite time, it eventually rolls back to the initial true minimum of the potential, around which it oscillates and thus drives the reheating. For illustration of these behaviors, we refer to fig. 5. These phase transitions in φ_3 triggered by φ_2 are the essential ingredient of our reheating mechanism.

Due to the approximate shift symmetry in the φ_2 direction, the system away from the NEC violation (and reheating) period realizes a phase of ghost condensation [25, 26] and the stress-energy tensor from $\mathcal{L}_{\text{NECV+reheat}}$ acts as an additional contribution to the c.c.. Without loss of generality, this additional contribution to the c.c. can be absorbed into $V_1(\varphi_1)$ so that the c.c. away from the NEC violation (and reheating) period is precisely V_1/M_{Pl}^2 .

While this process of the NEC violation and reheating is overall decoupled from the first scalar field φ_1 , one still has to be careful of the risk of overshooting. Indeed, the NEC violating and reheating eras break the simple relation (8) between the potential V_1 for φ_1 and the spacetime curvature, the latter of which controls the relation between Π_1 and $\dot{\varphi}_1$. During the NEC violation and reheating eras, the equation (7) for Π_1 is unchanged and thus $\Pi_1 = -c \times \mathcal{O}(1)$ still holds. On the other hand, $f(R)$ suddenly increases and affects the value of $\dot{\varphi}_1 = M_{\text{Pl}}^3 H^{-1} f \Pi_1$. As a result, the field φ_1 rolls down its potential V_1 faster and may overshoot the zero of V_1 . Because of this risk, the NEC-violating part should not last indefinitely; it needs to be constrained in time.

To better understand the issue at hand, let us consider the following calculations. Close to the zero of its potential V_1 , the field φ_1 follows a smooth evolution. Before the NEC violation and reheating, V_1 is (virtually) locked at a height of say $V_{\text{pre}} > 0$. To avoid a runaway down the potential into effectively negative c.c., the potential after the NEC violation and reheating, denoted as $V_{\text{after}} \equiv V_{\text{pre}} + \Delta V_1$, must stay above zero. We thus require

$$|\Delta V_1| < V_{\text{pre}} \quad (16)$$

during the NEC violation and reheating. One can easily estimate ΔV_1 as

$$\Delta V_1 \approx cM_{\text{Pl}}^3 \dot{\varphi}_1 \Delta t = -c^2 M_{\text{Pl}}^6 \frac{f}{H} \Delta t \times \mathcal{O}(1) = -c^2 M_{\text{Pl}}^6 \frac{f}{H} \frac{\Delta \varphi_2}{M^2} \times \mathcal{O}(1), \quad (17)$$

where Δt and $\Delta \varphi_2$ are the time duration and the corresponding field range of the NEC violating and reheating period, f is supposed to be estimated during this period, and we have assumed that the speed of φ_2 takes an approximately constant value, $\dot{\varphi}_2 \simeq M^2$. The last assumption will be explicitly confirmed by the example in section IV. Let us denote by V_2 ($\gg V_1$) the effective energy density of φ_2 , *i.e.* $V_2 \approx 3M_{\text{Pl}}^2 H^2$, during the NEC violation. Then, the condition of eq. (16) translates to a condition on $\Delta \varphi_2$, *i.e.* how long the NEC violation can last in the field space, namely, neglecting order-one numerical factors,

$$\frac{\Delta \varphi_2}{M} \lesssim \frac{M}{c^2 M_{\text{Pl}}} \left(\frac{M_{\text{Pl}}^4}{V_2} \right)^{(4m-1)/2} \frac{V_{\text{pre}}}{M_{\text{Pl}}^4}. \quad (18)$$

As the Universe experiences many sequences of the c.c. relaxation, NEC violation and reheating, this condition must be satisfied by every sequence all the way down to the last one before the present epoch that we live today, each time with a different (decreasing) value of V_{pre} . Barring accidental cancellation between V_{pre} and ΔV_1 for the last sequence, this requirement is fulfilled if and only if

$$\frac{\Delta \varphi_2}{M} \lesssim \frac{M}{c^2 M_{\text{Pl}}} \left(\frac{M_{\text{Pl}}^4}{V_2} \right)^{(4m-1)/2} \frac{\Lambda_{\text{obs}}}{M_{\text{Pl}}^2}, \quad (19)$$

where Λ_{obs} is the observed value of the cosmological constant, corresponding to the present value of the φ_1 potential $V_1|_{\text{now}} = M_{\text{Pl}}^2 \Lambda_{\text{obs}}$. Recalling that the parameter m must take a value $m > 3/2$, this result is suggestive in the sense that, no matter how large the NEC violation is, *i.e.* how large V_2 is, one can always achieve a sufficiently long period of it to support reheating for a sufficiently large value of m . We can thus pass over the overshooting problem.

III. NECV AND REHEATING SECTORS: BACKGROUND AND PERTURBATION

In this section we analyze the background system of the NEC-violating and reheating sectors and the perturbations around it, in order to find the parameter space in which it is stable against small perturbations. We do not include the c.c. relaxation sector φ_1 in the present analysis to avoid extra computational complexity; the φ_1 sector has supposedly decreased to a negligible amount by the time this analysis becomes relevant,⁴ provided that the condition (19) is satisfied. Hence the

⁴ For the analysis on the perturbative stability of the φ_1 sector alone, we would like to direct readers to [1, 2].

action of our interest in this section is

$$\begin{aligned} S &= \int d^4x \sqrt{-g} (\mathcal{L}_{\text{EH}} + \mathcal{L}_{\text{NECV+reheat}}) \\ &= \int d^4x \sqrt{-g} \left[\frac{M_{\text{Pl}}^2}{2} R + K(\varphi_2, X_2, \varphi_3) - G_3(\varphi_2, X_2, \varphi_3) \square \varphi_2 + P(\varphi_3, X_3) \right], \end{aligned} \quad (20)$$

where φ_2 and φ_3 are scalar fields for the NEC-violating and reheating sectors, respectively. We expand the two scalar fields as

$$\varphi_2(t, \mathbf{x}) = \bar{\varphi}_2(t) + \delta\varphi_2(t, \mathbf{x}), \quad \varphi_3 = \bar{\varphi}_3(t) + \delta\varphi_3(t, \mathbf{x}), \quad (21)$$

where $\bar{\varphi}_2(t)$ and $\bar{\varphi}_3(t)$ are the homogeneous background quantities, and $\delta\varphi_2$ and $\delta\varphi_3$ are their respective perturbations. For the spacetime metric we conduct the ADM decomposition

$$ds^2 = -N^2 dt^2 + \gamma_{ij} (N^i dt + dx^i) (N^j dt + dx^j), \quad (22)$$

where N and N^i are the lapse and shift functions, respectively, and γ_{ij} is the 3-D spatial metric. Note that these quantities contain $1+3+6=10$ variables, which fulfills the total number of variables in the spacetime metric. We decompose these variables into their background and perturbations as (we mainly adopt the notation in *e.g.* [18])

$$N(t, \mathbf{x}) = \bar{N}(t) [1 + \alpha(t, \mathbf{x})], \quad (23a)$$

$$N^i(t, \mathbf{x}) = \frac{\bar{N}(t)}{a(t)} [\partial_i \beta(t, \mathbf{x}) + B^i(t, \mathbf{x})], \quad (23b)$$

$$\begin{aligned} \gamma_{ij}(t, \mathbf{x}) &= a^2(t) e^{2\zeta(t, \mathbf{x})} \left[\delta_{ij} + 2 \partial_i \partial_j \mathcal{E}(t, \mathbf{x}) + 2 \partial_{(i} E_{j)}(t, \mathbf{x}) \right. \\ &\quad \left. + h_{ij}(t, \mathbf{x}) + \frac{1}{2} h_{ik}(t, \mathbf{x}) h_{kj}(t, \mathbf{x}) \right], \end{aligned} \quad (23c)$$

where \bar{N} and a are the background lapse and scale factor, respectively, $\{\alpha, \beta, \zeta, \mathcal{E}\}$ are scalar modes, the vector modes $\{B_i, E_i\}$ satisfy the transverse conditions $\partial_i B_i = \partial_i E_i = 0$, and the tensor modes $\{h_{ij}\}$ are transverse and traceless: $\partial_i h_{ij} = h_{ii} = 0$. This latter condition thus brings the number of degrees of freedom of the tensor sector from 6 to 2. Under the general coordinate transformation $x^\mu \rightarrow x^\mu + \xi^\mu(t, \mathbf{x})$, each variable transforms as

$$\begin{aligned} \Delta\alpha &= \frac{\partial_t(\bar{N}\xi^0)}{\bar{N}}, \quad \Delta\beta = \frac{a^3}{\bar{N}} \partial_t \xi_L - a \bar{N} \xi^0, \quad \Delta\zeta = H \bar{N} \xi^0, \quad \Delta\mathcal{E} = \xi_L, \\ \Delta B^i &= \frac{a}{\bar{N}} \partial_t \xi_T^i, \quad \Delta E_i = \xi_T^i, \quad \Delta h_{ij} = 0, \end{aligned} \quad (24)$$

and

$$\Delta\delta\varphi_2 = \partial_t \bar{\varphi}_2 \xi^0, \quad \Delta\delta\varphi_3 = \partial_t \bar{\varphi}_3 \xi^0, \quad (25)$$

where the decomposition $\xi^i = \delta^{ij} \partial_j \xi_L + \xi_T^i$ with $\partial_i \xi_T^i = 0$ has been used, and $H \equiv \partial_t a / (a \bar{N})$ is the Hubble expansion rate. Using the previous symmetry and appropriately choosing ξ^μ , we fix the gauge by setting

$$\delta\varphi_2 = \mathcal{E} = E_i = 0, \quad \text{gauge fixing}, \quad (26)$$

leaving no further gauge freedom. Then at the level of linear perturbations, the remaining vector modes B^i are non-dynamical and fixed to null by constraints, and they can hence be omitted from our discussion altogether. Thus our system of perturbations consists of the two sectors

$$\begin{cases} \alpha, \beta, \zeta, \delta\varphi_3 & : \text{scalar sector}, \\ h_{ij} & : \text{tensor sector}. \end{cases} \quad (27)$$

Among the scalar variables, α and β are non-dynamical, and their values are fixed by the dynamical modes ζ and $\delta\varphi_3$. Therefore, each of the scalar and tensor sectors is a system of 2 propagating degrees of freedom. In particular, thanks to the background rotational symmetry, these sectors are decoupled at the level of the quadratic action,⁵ *i.e.*

$$S^{(2)} = S_{\text{scalar}}[\alpha, \beta, \zeta, \delta\varphi_3] + S_{\text{tensor}}[h]. \quad (28)$$

In the following subsections, we formally derive the background equations of this two-scalar system and the stability conditions against perturbations.⁶

A. Background equations

The background quantities, defined in eqs. (21) and (23), obey their classical equations of motion (e.o.m.), which are obtained by varying the action eq. (20) with respect to each of them. In order to avoid crowded notations, we here take $\bar{N} = 1$ and omit the bars over background quantities in this subsection. The e.o.m.'s then read

$$\begin{aligned} 0 = & -\partial_{X_2} K \dot{\varphi}_2^2 - \partial_{X_3} P \dot{\varphi}_3^2 + \partial_{\varphi_3} G_3 \dot{\varphi}_3 \dot{\varphi}_2 + \partial_{\varphi_2} G_3 \dot{\varphi}_2^2 + K + P \\ & - 3H \partial_{X_2} G_3 \dot{\varphi}_2^3 + 3M_{\text{Pl}}^2 H^2, \end{aligned} \quad (29a)$$

$$0 = -\dot{\varphi}_2 [\partial_{\varphi_3} G_3 \dot{\varphi}_3 + \dot{\varphi}_2 (\partial_{X_2} G_3 \dot{\varphi}_2 + \partial_{\varphi_2} G_3)] + K + P + M_{\text{Pl}}^2 (2\dot{H} + 3H^2), \quad (29b)$$

⁵ Note that the linear action only derives the background equations and gives no information about perturbations.

⁶ For derivation of the equations for the background as well as perturbations, we refer to [18] for a detailed calculations of a single-field case and to [27] for a general multi-field extension.

$$\begin{aligned}
0 = & -3 \partial_{X_2} G_3 \left(\dot{H} + H^2 \right) \dot{\varphi}_2^2 - 6H^2 \partial_{X_2} G_3 \dot{\varphi}_2^2 + \partial_{\varphi_2 X_2} G_3 \dot{\varphi}_2^2 \ddot{\varphi}_2 + \partial_{\varphi_2 \varphi_2} G_3 \dot{\varphi}_2^2 \\
& - 3H \left\{ \dot{\varphi}_2 \left[\partial_{X_2} K + \ddot{\varphi}_2 \left(\partial_{X_2 X_2} G_3 \dot{\varphi}_2^2 + 2 \partial_{X_2} G_3 \right) + \partial_{\varphi_2 X_2} G_3 \dot{\varphi}_2^2 - 2 \partial_{\varphi_2} G_3 \right] \right. \\
& \left. + \dot{\varphi}_3 \left(\partial_{X_2 \varphi_3} G_3 \dot{\varphi}_2^2 - \partial_{\varphi_3} G_3 \right) \right\} - \partial_{X_2 X_2} K \dot{\varphi}_2^2 \ddot{\varphi}_2 - \partial_{\varphi_2 X_2} K \dot{\varphi}_2^2 - \partial_{X_2} K \ddot{\varphi}_2 + \partial_{\varphi_2} K \\
& + \dot{\varphi}_3 \dot{\varphi}_2 \left(-\partial_{X_2 \varphi_3} K + \partial_{X_2 \varphi_3} G_3 \ddot{\varphi}_2 + 2 \partial_{\varphi_2 \varphi_3} G_3 \right) + \partial_{\varphi_3 \varphi_3} G_3 \dot{\varphi}_3^2 + \partial_{\varphi_3} G_3 \ddot{\varphi}_3 \\
& + 2 \partial_{\varphi_2} G_3 \ddot{\varphi}_2 ,
\end{aligned} \tag{29c}$$

$$\begin{aligned}
0 = & \partial_{\varphi_3} K - \ddot{\varphi}_3 \left(\partial_{X_3 X_3} P \dot{\varphi}_3^2 + \partial_{X_3} P \right) - \partial_{\varphi_3 X_3} P \dot{\varphi}_3^2 + \partial_{\varphi_3} P \\
& + 3H \left(\partial_{\varphi_3} G_3 \dot{\varphi}_2 - \partial_{X_3} P \dot{\varphi}_3 \right) + \partial_{\varphi_3} G_3 \ddot{\varphi}_2 .
\end{aligned} \tag{29d}$$

The first eq. (29a) is a constraint equation, and the remaining three equations constitute a system of second-order differential equations for φ_2 , φ_3 and a that shall be numerically solved in section V.

We note that, in section IV, we restrict our interest to seeking the solution of the NEC-violating sector that gives $X_2 = \text{constant}$, *i.e.* $\varphi_2 \propto t$, in the absence of φ_3 . This ansatz greatly simplifies the search of required forms of the functions K , G_3 and P to achieve the target cosmic history as shown in fig. 1 (or fig. 2 in the absence of φ_3). Before proceeding to the reconstruction procedure of those functions that is described in detail in section IV, we collect the conditions necessary to ensure our background solution to be stable against small perturbations in the following subsections.

B. Perturbations

In this subsection we analyze the stability of the NEC violation and reheating sector against perturbations. As described at the beginning of this section, we decompose the perturbations of the fields and metric as in eqs. (21) and (23), respectively, and fix the gauge freedom as in eq. (26). At the level of linear perturbations, the scalar, vector and tensor sectors are mutually decoupled, thanks to the background rotational symmetry, and the vector sector contains no dynamical degree of freedom. We thus need only to study the decoupled scalar and tensor perturbations as in eq. (28), which is done separately hereafter.

1. Tensor sector

The tensor sector takes the standard form, that is, the action of the type shown in eq. (20) (without non-trivial G_4 or G_5 term in the Horndeski theory) leads to the same form of S_{tensor} as

the one of General Relativity, *i.e.*

$$S_{\text{tensor}} = \frac{M_{\text{Pl}}^2}{8} \int \bar{N} dt a^3 d^3x \left[\frac{\partial_t h_{ij} \partial_t h_{ij}}{\bar{N}^2} - \frac{\partial_k h_{ij} \partial_k h_{ij}}{a^2} \right], \quad (30)$$

where the background lapse \bar{N} is put back.⁷ The tensor sector is here trivially free from ghost and gradient instabilities. Therefore, we shall simply focus on the stability conditions in the scalar perturbations.

2. Scalar sector

The scalar sector consists of 4 variables $\{\alpha, \beta, \zeta, \delta\varphi_3\} \equiv q$, where α and β are non-dynamical and do not have their own kinetic terms, as explained around eq. (27). Fourier-transforming each variable as

$$q(t, \mathbf{x}) = \int \frac{d^3k}{(2\pi)^{3/2}} e^{i\mathbf{k}\cdot\mathbf{x}} \hat{q}(t, \mathbf{k}), \quad (31)$$

with hat $\hat{\cdot}$ denoting Fourier-transformed quantities, the quadratic action S_{scalar} can be formally written in the form

$$S_{\text{scalar}} = \frac{1}{2} \int dt d^3k \left[\partial_t \hat{\delta}^\dagger A \partial_t \hat{\delta} + \left(\partial_t \hat{\delta}^\dagger B \hat{\delta} + \text{h.c.} \right) + \hat{\delta}^\dagger C \hat{\delta} \right. \\ \left. + \hat{\mathcal{N}}^\dagger D \hat{\mathcal{N}} + \left(\hat{\mathcal{N}}^\dagger E \partial_t \hat{\delta} + \text{h.c.} \right) + \left(\hat{\mathcal{N}}^\dagger F \hat{\delta} + \text{h.c.} \right) \right], \quad (32)$$

up to total derivatives, where $\hat{\delta} = \{\hat{\zeta}, \delta\hat{\varphi}_3\}$ and $\hat{\mathcal{N}} = \{\hat{\alpha}, \hat{\beta}\}$ are arrays grouping the dynamical and non-dynamical variables, respectively. Note that the reality condition of the variables in the coordinate space is translated to $\hat{q}^\dagger(\mathbf{k}) = \hat{q}(-\mathbf{k})$ in the Fourier space. The coefficients A, B, C, D, E and F are all 2×2 square matrices whose components consist of the background quantities, explicitly

$$A = \frac{a^3}{N} \begin{pmatrix} -6M_{\text{Pl}}^2 & 0 \\ 0 & \mathcal{G}_\varphi \end{pmatrix}, \quad B = a^3 \begin{pmatrix} 0 & \frac{3}{2}c_1 \\ -\frac{3}{2}c_1 & 0 \end{pmatrix}, \\ C = Na^3 \begin{pmatrix} 2M_{\text{Pl}}^2 \frac{k^2}{a^2} & \frac{3}{2}c_2 \\ \frac{3}{2}c_2 & -\frac{k^2}{a^2} (\mathcal{G}_\varphi - 2X_3 \partial_{X_3 X_3} P) + c_3 \end{pmatrix}, \quad D = Na^3 \begin{pmatrix} 2\Sigma + \frac{c_4^2}{\mathcal{G}_\varphi} & \frac{2k^2}{a} \Theta \\ \frac{2k^2}{a} \Theta & 0 \end{pmatrix}, \quad (33) \\ E = a^3 \begin{pmatrix} 6\Theta & c_4 \\ -2M_{\text{Pl}}^2 \frac{k^2}{a} & 0 \end{pmatrix}, \quad F = Na^3 \begin{pmatrix} 2M_{\text{Pl}}^2 \frac{k^2}{a^2} & c_5 \\ 0 & \frac{k^2}{a} c_1 \end{pmatrix},$$

⁷ In deriving the expression of eq. (30), the background equations are not used, which is the benefit of defining h_{ij} by adding the quadratic term of h_{ij} in eq. (23c). Without it, the same form of S_{tensor} can be derived, but only after the background equations are imposed.

where

$$\mathcal{G}_\varphi = \partial_{X_3} P + 2X_3 \partial_{X_3 X_3} P, \quad (34)$$

$$\begin{aligned} \Sigma = & -3M_{\text{Pl}}^2 H^2 - \frac{X_2 (\partial_{\varphi_3} G_3)^2}{\mathcal{G}_\varphi} + X_2 \left(\partial_{X_2} K + 2X_2 \partial_{X_2 X_2} K - 2 \partial_{\varphi_2} G_3 \right. \\ & \left. + 12H \frac{\dot{\varphi}_2}{N} \partial_{X_2} G_3 - 2X_2 \partial_{\varphi_2 X_2} G_3 + 6H \frac{\dot{\varphi}_2}{N} X_2 \partial_{X_2 X_2} G_3 - \frac{\dot{\varphi}_2 \dot{\varphi}_3}{N^2} \partial_{X_2 \varphi_3} G_3 \right), \end{aligned} \quad (35)$$

$$\Theta = M_{\text{Pl}}^2 H - \frac{\dot{\varphi}_2}{N} X_2 \partial_{X_2} G_3 \quad (36)$$

$$c_1 = \frac{\dot{\varphi}_2}{N} \partial_{\varphi_3} G_3 - \frac{\dot{\varphi}_3}{N} \partial_{X_3} P, \quad (37)$$

$$\begin{aligned} c_2 = & - \left[\frac{1}{N} \partial_t \left(\frac{\dot{\varphi}_2}{N} \right) + 3H \frac{\dot{\varphi}_2}{N} \right] \partial_{\varphi_3} G_3 - \frac{2}{N} \partial_t \left(\frac{\dot{\varphi}_2}{N} \right) X_2 \partial_{X_2 \varphi_3} G_3 - 2X_2 \partial_{\varphi_2 \varphi_3} G_3 \\ & - \frac{\dot{\varphi}_2 \dot{\varphi}_3}{N^2} \partial_{\varphi_3 \varphi_3} G_3 + \left[\frac{1}{N} \partial_t \left(\frac{\dot{\varphi}_3}{N} \right) + 3H \frac{\dot{\varphi}_3}{N} \right] \partial_{X_3} P + \frac{2}{N} \partial_t \left(\frac{\dot{\varphi}_3}{N} \right) X_3 \partial_{X_3 X_3} P \\ & + 2X_3 \partial_{\varphi_3 X_3} P, \end{aligned} \quad (38)$$

$$\begin{aligned} c_3 = & \partial_{\varphi_3 \varphi_3} K + \left[\frac{1}{N} \partial_t \left(\frac{\dot{\varphi}_2}{N} \right) + 3H \frac{\dot{\varphi}_2}{N} \right] \partial_{\varphi_3 \varphi_3} G_3 + \partial_{\varphi_3 \varphi_3} P - 2X_3 \partial_{\varphi_3 \varphi_3 X_3} P \\ & - \left[\frac{1}{N} \partial_t \left(\frac{\dot{\varphi}_3}{N} \right) + 3H \frac{\dot{\varphi}_3}{N} \right] \partial_{\varphi_3 X_3} P - \frac{2}{N} \partial_t \left(\frac{\dot{\varphi}_3}{N} \right) X_3 \partial_{\varphi_3 X_3 X_3} P, \end{aligned} \quad (39)$$

$$c_4 = \frac{\dot{\varphi}_2}{N} \partial_{\varphi_3} G_3 - \frac{\dot{\varphi}_3}{N} \mathcal{G}_\varphi, \quad (40)$$

$$\begin{aligned} c_5 = & -2X_2 \partial_{X_2 \varphi_3} K - \left[\frac{1}{N} \partial_t \left(\frac{\dot{\varphi}_2}{N} \right) + 3H \frac{\dot{\varphi}_2}{N} \right] \partial_{\varphi_3} G_3 \\ & - 6H \frac{\dot{\varphi}_2}{N} X_2 \partial_{X_2 \varphi_3} G_3 + 2X_2 \partial_{\varphi_2 \varphi_3} G_3 + \frac{\dot{\varphi}_2 \dot{\varphi}_3}{N^2} \partial_{\varphi_3 \varphi_3} G_3 \\ & + \left[\frac{1}{N} \partial_t \left(\frac{\dot{\varphi}_3}{N} \right) + 3H \frac{\dot{\varphi}_3}{N} \right] \partial_{X_3} P + \frac{2}{N} \partial_t \left(\frac{\dot{\varphi}_3}{N} \right) X_3 \partial_{X_3 X_3} P, \end{aligned} \quad (41)$$

noting that the bar $\bar{}$ is here omitted from the background quantities to avoid crowded notation.

By varying the action of eq. (32) with respect to $\hat{\mathcal{N}}^\dagger$, we find the constraint equations that fix the non-dynamical variables in terms of the dynamical ones δ , given by

$$\hat{\mathcal{N}} = -D^{-1} \left(E \partial_t \hat{\delta} + F \hat{\delta} \right), \quad (42)$$

as $\det(D) \neq 0$ in our current system. Plugging this back into eq. (32), we obtain the action in terms only of the dynamical degrees of freedom,

$$S_{\text{scalar}} = \frac{1}{2} \int dt d^3k \left[\partial_t \hat{\delta}^\dagger \tilde{A} \partial_t \hat{\delta} + \left(\partial_t \hat{\delta}^\dagger \tilde{B} \hat{\delta} + \text{h.c.} \right) + \hat{\delta}^\dagger \tilde{C} \hat{\delta} \right], \quad (43)$$

where

$$\tilde{A} = A - E^\dagger D^{-1} E, \quad \tilde{B} = B - E^\dagger D^{-1} F, \quad \tilde{C} = C - F^\dagger D^{-1} F. \quad (44)$$

Notice that now the kinetic matrix \tilde{A} is no longer diagonal. In order to diagonalize it, we can perform the following change of variables,

$$\hat{\delta} = R\hat{\Delta}, \quad R = \begin{pmatrix} 1 & 0 \\ -\frac{M_{\text{Pl}}^2 c_4}{\mathcal{G}_\varphi \Theta} & 1 \end{pmatrix}, \quad (45)$$

which results in the action in terms of $\hat{\Delta}$,

$$S_{\text{scalar}} = \frac{1}{2} \int dt d^3k \left[\partial_t \hat{\Delta}^\dagger \tilde{T} \partial_t \hat{\Delta} + \left(\partial_t \hat{\Delta}^\dagger \tilde{X} \hat{\Delta} + \text{h.c.} \right) - \hat{\Delta}^\dagger \tilde{\Omega}^2 \hat{\Delta} \right], \quad (46)$$

where

$$\begin{aligned} \tilde{T} &= R^\dagger \tilde{A} R, \\ \tilde{X} &= R^\dagger \tilde{B} R + R^\dagger \tilde{A} \partial_t R, \\ \tilde{\Omega}^2 &= -R^\dagger \tilde{C} R - \partial_t R^\dagger \tilde{A} \partial_t R - \partial_t R^\dagger \tilde{B} R - R^\dagger \tilde{B}^\dagger \partial_t R. \end{aligned} \quad (47)$$

Finally, by adding the total derivative $-\frac{1}{4} \int dt d^3k (\tilde{X} + \tilde{X}^\dagger)$, we arrive at the final expression for the quadratic action

$$S_{\text{scalar}} = \frac{1}{2} \int dt d^3k \left[\partial_t \hat{\Delta}^\dagger T \partial_t \hat{\Delta} + \partial_t \hat{\Delta}^\dagger X \hat{\Delta} - \hat{\Delta}^\dagger X \partial_t \hat{\Delta} - \hat{\Delta}^\dagger \Omega^2 \hat{\Delta} \right], \quad (48)$$

where

$$T = \tilde{T}, \quad X = \frac{\tilde{X} - \tilde{X}^\dagger}{2}, \quad \Omega^2 = \tilde{\Omega}^2 + \frac{\partial_t \tilde{X} + \partial_t \tilde{X}^\dagger}{2}. \quad (49)$$

Note that T and Ω^2 are symmetric 2×2 matrices, and X is an anti-symmetric one. Now the kinetic matrix

$$T = \frac{a^3}{N} \begin{pmatrix} 2M_{\text{Pl}}^2 \mathcal{G}_S & 0 \\ 0 & \mathcal{G}_\varphi \end{pmatrix}, \quad \mathcal{G}_S \equiv 3 + M_{\text{Pl}}^2 \frac{\Sigma}{\Theta^2}, \quad (50)$$

is diagonal, as desired. The conditions to prohibit ghost instabilities are therefore

$$\mathcal{G}_S > 0, \quad \mathcal{G}_\varphi > 0, \quad \text{no ghost}, \quad (51)$$

serving as part of the conditions of perturbative stability (\mathcal{G}_φ is defined in eq. (34)).

Another instability we need to suppress is the gradient instability. We are only concerned with high-momentum catastrophic instability, as the low-momentum counterpart may be harmless at a non-linear level *à la* Jeans instability. This amounts to imposing positivity condition for the squared sound speeds of the scalar perturbations, c_s^2 , as defined below. In the high- k limit, we

collect the terms in the coefficient matrices of the order $T \sim \mathcal{O}(k^0)$, $X \sim \mathcal{O}(k^1)$ and $\Omega^2 \sim \mathcal{O}(k^2)$. The full expression of T is given in eq. (50) and does not depend on k . The other matrices in the high- k limit read

$$X = 0 + \mathcal{O}(k^0), \quad \Omega^2 = \Omega_{\mathcal{O}(k^2)}^2 + \mathcal{O}(k^0), \quad (52)$$

where $\Omega_{\mathcal{O}(k^2)}^2$ only contains the terms proportional to k^2 in the high- k limit. Taking the ansatz $\hat{\Delta} \propto \exp\left(i \int^t N dt' c_s k/a\right)$ as an adiabatic solution for large k , the sound speed c_s^2 can be found by solving the characteristic equation

$$\det\left(-c_s^2 k^2 \frac{N^2}{a^2} T + \Omega^2\right) = 0, \quad (53)$$

leading to

$$c_s^4 - \left(c_\chi^2 + \frac{\mathcal{F}_S}{\mathcal{G}_S} + \mathcal{A} + \mathcal{B}\right) c_s^2 + c_\chi^2 \left(\frac{\mathcal{F}_S}{\mathcal{G}_S} + \mathcal{A}\right) = 0, \quad (54)$$

where

$$\begin{aligned} \mathcal{F}_S &\equiv \frac{M_{\text{Pl}}^4}{Na} \partial_t \left(\frac{a}{\Theta}\right) - M_{\text{Pl}}^2, & c_\chi^2 &\equiv \frac{\partial_{X_3} P}{\partial_{X_3} P + 2X_3 \partial_{X_3 X_3} P}, \\ \mathcal{A} &\equiv -\frac{M_{\text{Pl}}^4}{2\partial_{X_3} P \mathcal{G}_S \Theta^2} \left(\frac{\dot{\varphi}_2}{N} \partial_{\varphi_3} G_3 - \frac{\dot{\varphi}_3}{N} \partial_{X_3} P\right)^2, & \mathcal{B} &\equiv \frac{4M_{\text{Pl}}^4 X_2 X_3^2 (\partial_{X_3 X_3} P)^2 (\partial_{\varphi_3} G_3)^2}{\partial_{X_3} P \mathcal{G}_S \mathcal{G}_\varphi^2 \Theta^2}. \end{aligned} \quad (55)$$

The values of c_s^2 are determined by the two roots of eq. (54), and we impose the conditions

$$c_s^2 > 0, \quad \text{gradient stability}, \quad (56)$$

for each value of c_s^2 .

Notice from eq. (54) that, in the particular cases of $\partial_{\varphi_3} G_3 = 0$ and/or $\partial_{X_3 X_3} P = 0$, we have $\mathcal{B} = 0$, and the expressions of c_s^2 vastly simplify. In our numerical examples, we indeed take

$$\partial_{\varphi_3} G_3 = 0 \quad \& \quad \partial_{X_3 X_3} P = 0, \quad \text{numerical examples}, \quad (57)$$

and in this case

$$c_s^2 = c_\chi^2 \quad \text{or} \quad c_s^2 = \frac{\mathcal{F}_S}{\mathcal{G}_S} + \mathcal{A}, \quad (58)$$

while

$$c_\chi^2 = 1, \quad \mathcal{A} = -\frac{M_{\text{Pl}}^4 X_3 \partial_{X_3} P}{\mathcal{G}_S \Theta^2}. \quad (59)$$

Therefore, in these particular examples, we only need to impose

$$\mathcal{F}_S > \frac{M_{\text{Pl}}^4 X_3 \partial_{X_3} P}{\Theta^2}, \quad (60)$$

to avoid gradient instability, as we have already imposed $\mathcal{G}_S > 0$ from the no-ghost condition. In summary, to ensure the background evolution to be stable against small perturbations, we impose the conditions in eqs. (51) and (56), or those in eqs. (51) and (60) for the particular and simpler examples, for the entire history of the Universe, and particularly during the phases of NEC violation and reheating.

IV. A CONCRETE IMPLEMENTATION

We have until now kept arbitrary the free functions $f_{1,2}(\varphi_2, \varphi_3)$, $f(\varphi_2, \varphi_3)$, $V(\varphi_2, \varphi_3)$ and $U(\varphi_3)$ in the NEC violating and reheating Lagrangian $\mathcal{L}_{\text{NECV+reh}}$, eq. (11), but we now choose a concrete set of functions to fully realise our desired cosmological scenario. For the purpose of the conceptual proof, we take an inverted route: we first determine a desired cosmic history we would like to achieve, which is summarized in section II, and then reconstruct the functions accordingly. While we disregard the reheating field φ_3 in this procedure, we numerically verify the overall behavior of the whole system after reviving the φ_3 dependence into the reconstructed model.

A. Reconstruction of the NEC-violating sector

We have a total of 3 independent functions, K , G_3 and P , and expand K and G_3 as polynomial functions of X_2 as in eq. (13). To reconstruct them, we first consider the NEC-violating sector alone by turning off the φ_3 and disregarding $P(\varphi_3, X_3)$. On the one hand, there are 4 independent functions, $\tilde{f}_1(\varphi_2)$, $\tilde{f}_2(\varphi_2)$ and $\tilde{V}(\varphi_2)$ from \tilde{K} , and $\tilde{f}(\varphi_2)$ from \tilde{G}_3 (recall tilde denotes quantities with φ_3 dependence taken out). On the other hand, we have 2 independent background equations from eq. (29) (with φ_3 turned off). Therefore, the forms of two of these functions can be fixed by the background equations, once all other arbitrary functions are chosen by hand. In the following we reconstruct these functions in the action so that the system admits the following solution,

$$H = H_{\text{necv}}(\varphi_2), \quad \varphi_2 = t, \quad \bar{N} = 1, \quad (61)$$

where H is the Hubble expansion rate and $H_{\text{necv}}(\varphi_2)$ is a fixed function corresponding to the input Hubble expansion rate.

The NEC-violating sector is assumed to be periodic in the field value of φ_2 , as discussed in section II B. Without loss of generality, we shift φ_2 such that the NEC-violating (and reheating) period is localized around $\varphi_2 = 0$. We then take the following ansatz for the forms of \tilde{K} and G_3 ,

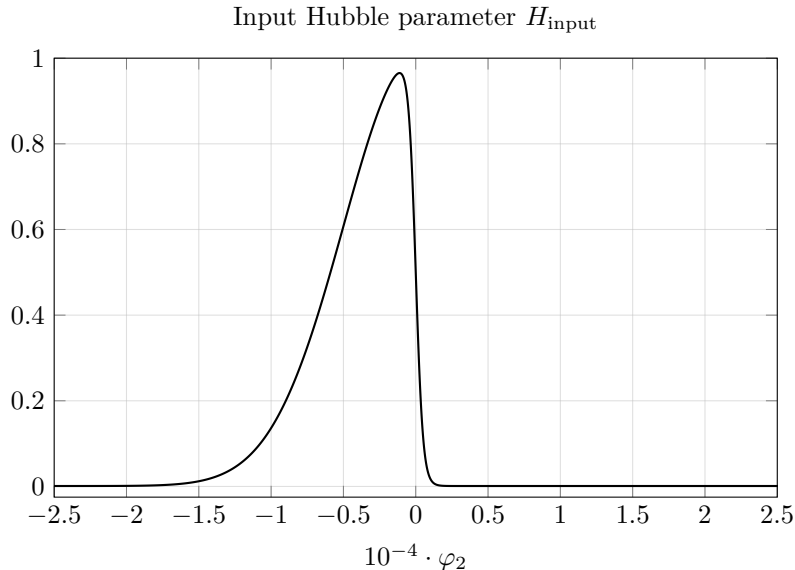


Figure 3. Overall shape of the input Hubble expansion rate H_{necv} . The plot uses the numerical parameters exhibited in table I.

that is,

$$\tilde{K} = M_{\text{Pl}}^2 H_{\text{dip}}^2 \left[F_1(\varphi_2) X_2 + F_2(\varphi_2) X_2^2 - v(\varphi_2) \right], \quad v(\varphi_2) = -v_0 \exp\left(-\frac{\varphi_2^2}{2T_{\text{dip}}^2}\right), \quad (62a)$$

$$\tilde{G}_3 = M_{\text{Pl}}^2 H_{\text{necv}}(\varphi_2) F_{\text{kb}}(\varphi_2) X_2, \quad F_{\text{kb}}(\varphi_2) = F_{\text{kb},0} + F_{\text{kb},1} \exp\left(-\frac{\varphi_2^2}{2T_{\text{kb}}^2}\right), \quad (62b)$$

where H_{dip} is a constant of mass dimension 1, T_{dip} and T_{kb} of mass dimension -1 , and v_0 , $F_{\text{kb},0}$ and $F_{\text{kb},1}$ are dimensionless constants. We here normalize φ_2 so that it has mass dimension -1 , and thus X_2 is dimensionless. The functions F_1 , F_2 and F_{kb} correspond to \tilde{f}_1 , \tilde{f}_2 and \tilde{f} (eq. (13)), respectively, that are made dimensionless. The potential v has a ‘dip’ of depth v_0 at $\varphi_2 = 0$ so that φ_2 can be trapped to sustain a NEC-violating period. The \tilde{G}_3 contribution is needed to ensure the stability of the system in this period. For this reason, we use the input Hubble expansion rate $H_{\text{necv}}(\varphi_2)$ as an overall factor of \tilde{G}_3 so that the \tilde{G}_3 contribution becomes prominent in the NEC violating phase.

For the actual form of H_{necv} that we employ, we introduce two scales to turn on and off NEC violation. There are many possible forms to achieve this, and we simply take one particular choice, *i.e.*

$$H_{\text{necv}}(\varphi_2) = H_0 + H_1 \exp\left(-\frac{\varphi_2^2}{2T^2}\right) \frac{1 - \tanh\left(\frac{\varphi_2}{\tau}\right)}{2}, \quad (63)$$

where H_0 and H_1 are constants of dimension 1, while T and τ those of dimension -1 . The value of H_{necv} far away from the origin (*i.e.* $|\varphi_2| \gg T, \tau$) is H_0 , that is during a major duration of the cosmic

history, and is essentially the present value of the Hubble expansion rate if we apply this system to the last NEC violating phase before the present epoch of the Universe. However, during the NEC violating phase, it ascends to the maximum value $\sim H_0 + H_1$ within a time scale controlled by T , eventually going through a step-function-like drop around $\varphi_2 = 0$ to H_0 with another scale controlled by τ . The overall shape of H_{necv} is graphically depicted in fig. 3. In practice, the drop needs to be sharper than the rise ($T \gg \tau$) in order to accommodate a reheating period toward the end of the NEC violation by transferring a large portion of the energy in φ_2 abruptly enough so that the reheating field φ_3 starts oscillating using the transferred energy.

We now have all the setups for the reconstruction. In order to ensure the target cosmic history of eq. (63) to be compatible with time evolution, we seek for a solution of the form eq. (61). We then substitute eq. (61) and eq. (62) into the background equations of motion in eq. (29). Only two of the equations are independent when φ_3 is turned off, and they give

$$F_1 = 4v + 3(F_{\text{kb}} - 4) \frac{H_{\text{necv}}^2}{H_{\text{dip}}^2} + \frac{F'_{\text{kb}} H_{\text{necv}}}{H_{\text{dip}}^2} + (F_{\text{kb}} - 6) \frac{H'_{\text{necv}}}{H_{\text{dip}}^2}, \quad (64a)$$

$$F_2 = -4v - 6(F_{\text{kb}} - 2) \frac{H_{\text{necv}}^2}{H_{\text{dip}}^2} + \frac{4H'_{\text{necv}}}{H_{\text{dip}}^2}, \quad (64b)$$

where prime denotes $\partial/\partial t = \partial/\partial\varphi_2$ under eq. (61). Recovering φ_2 dependence by basically replacing $t \rightarrow \varphi_2$, these two equations fix the forms of F_1 and F_2 , given the predetermined functions H_{necv} , F_{kb} and v . This completes the reconstruction of the NEC-violating sector for our concrete implementation of the model.

B. Attractor behavior of the NEC-violating dynamics

We have fixed the forms of the model functions in the φ_2 sector as eq. (64) so that the NEC violation as depicted in eq. (63) and eq. (61) is achieved as a solution of the background equations of motion. However whether or not this particular solution is an attractor of the dynamical system is a separate issue, which we would like to address in this subsection. The analysis here concerns the background eq. (29) with the reconstructed functions of eq. (62) with eqs. (63) and (64).

We first perform a linearized analysis, and to this end we expand the background quantities as

$$\varphi_2(t) = \varphi^{(0)}(t) + \epsilon \varphi^{(1)}(t), \quad H(t) = H^{(0)}(t) + \epsilon H^{(1)}(t), \quad (65)$$

where $\varphi^{(0)} = t$ and $H^{(0)} = H_{\text{necv}}(t)$ denote the solutions assumed for the reconstruction in the previous subsection while $\epsilon\varphi^{(1)}$ and $\epsilon H^{(1)}$ are small perturbations, and ϵ is the expansion parameter. We then expand the background eq. (29) up to the linear order in ϵ . The $\mathcal{O}(\epsilon^0)$ equations are

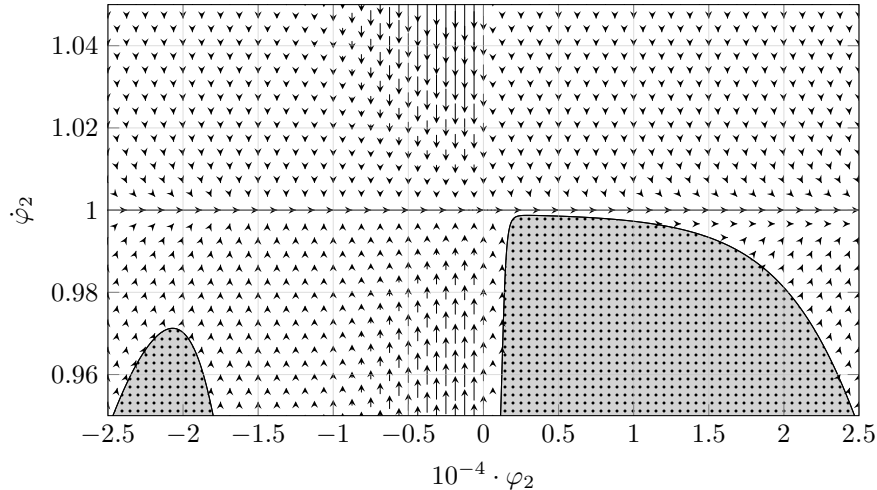


Figure 4. The phase portrait of φ_2 and $\dot{\varphi}_2$ as a vector field. Arrows are scaled proportionally to the gradient intensity. The above plot therefore exhibits the strong attraction to the solution $\varphi_2 \equiv t$, especially in the central area (between approximately $\varphi_2 = -5000$ and 0). The lightly shaded regions are where H takes a complex value as a solution to the constraint eq. (29a), that is where a real background solution does not exist.

trivially satisfied, and the $\mathcal{O}(\epsilon^1)$ equation for $H^{(1)}$ is a constraint equation that can be solved for $H^{(1)}$ in favor of $\varphi^{(1)}(t)$ and $\partial_t \varphi^{(1)}$. As a result, the master equation of the linearized system is only in terms of $\varphi^{(1)}$ with $\mathcal{O}(\epsilon^0)$ coefficients, and reducing it to a coupled system of first-order equations gives, in a matrix form,

$$\partial_t \begin{pmatrix} \varphi^{(1)} \\ \pi_\varphi^{(1)} \end{pmatrix} = \mathcal{M} \begin{pmatrix} \varphi^{(1)} \\ \pi_\varphi^{(1)} \end{pmatrix}, \quad \mathcal{M} = \begin{pmatrix} 0 & 1 \\ \mathcal{A} & \mathcal{B} \end{pmatrix}, \quad (66)$$

where \mathcal{A} and \mathcal{B} are functions of the $\mathcal{O}(\epsilon^0)$ quantities. While \mathcal{A} and \mathcal{B} are in general of lengthy expressions, our restriction of including only up to the \mathcal{L}_3 terms of Horndeski theory with the e.o.m.-consistent reconstructed functions of eq. (62) conveniently sets $\mathcal{A} = 0$. Hence, the eigenvalues of the matrix \mathcal{M} are 0 and \mathcal{B} . In order for the solutions $\varphi^{(0)} = t$ and $H^{(0)} = H_{\text{necv}}(t)$ to be a local attractor of the system, we thus require these eigenvalues be non-positive, *i.e.*⁸

$$\mathcal{B} \leq 0. \quad (67)$$

This ensures the local stability of the solution assumed in the previous subsection.

⁸ In principle the non-positiveness condition could be imposed only on the real part of the eigenvalues. However, the components of \mathcal{B} (and \mathcal{A}) consist of the $\mathcal{O}(\epsilon^0)$ quantities, and the only occasion in which they become complex is when the value of $H^{(0)}$ becomes complex as a solution of the constraint equation, but this only means that there is no real solution at the $\mathcal{O}(\epsilon^0)$ order. We exclude such a case.

The previous analysis is a linearized one, and in order to observe a more global behavior of the system, we resort to a numerical phase-space illustration, a representative case of which is depicted in fig. 4. As seen in the figure, $\varphi_2 = t$, which is our input solution for the reconstruction, is indeed the global attractor of the system. This justifies our ansatz and reconstruction of the model functions in the previous subsection, and the system is resistant against small perturbations at least in the direction of positive $\dot{\varphi}_2$. In fig. 4, the values of H_0 , which is essentially the Hubble expansion rate at present, is taken rather close to that of H_1 , which corresponds to the amount of raise in H during the NEC violating phase, for numerical ease. When the hierarchy between these values is closer to a realistic one, we note two cautions. First, the shaded complex regions approach closer to the $\dot{\varphi}_2$ line. However they never cross it provided taking sufficiently large value of v_0 . Second, when H_0 becomes much smaller than H_1 , the attractor behavior towards the input solution $\varphi_2 = t$ is rather weak away from the NEC-violating region. Indeed, in a small H_0 limit and sufficiently far from the NEC violation so that $v \approx 0$ and $F_{\text{kb}} \approx F_{\text{kb},0}$, the value of \mathcal{B} takes

$$\mathcal{B} \simeq -3H_0, \quad H_0 \ll H_1, \quad (68)$$

which makes the validity of the solution $\varphi_2 = t$ somewhat worrisome. However, it is still a local attractor because $\mathcal{B} < 0$. Moreover, we are assuming a period of the NEC-preserving phase much longer than that of the NEC-violating one. Therefore, even though the attractor appears to be weak in the limit $H_0 \ll H_1$, the background system is expected to go back to the solution $\varphi_2 = t$ during the long NEC-preserving era.

C. Recovering the reheating sector coupled to NEC violation

To realize the known big bang universe after the NEC-violating era, the reheating field φ_3 necessarily couples to φ_2 in a non-minimal manner. Our choice of the coupling amounts to making the following replacements:

$$F_1 \rightarrow \frac{1 + \alpha_{\text{kick}} e^{-\beta_{\text{kick}} \varphi_3}}{1 + \alpha_{\text{kick}}} F_1, \quad (69a)$$

$$F_2 \rightarrow \frac{1 + \alpha_{\text{kick}} e^{-\beta_{\text{kick}} \varphi_3}}{1 + \alpha_{\text{kick}}} F_2, \quad (69b)$$

$$v \rightarrow \exp \left[-\beta_{\text{dip}}^2 \left((\varphi_3 - 1)^2 - 1 \right) \right] v, \quad (69c)$$

while we reintroduce the kinetic term and bare potential of φ_3 as

$$P(\varphi_3, X_3) = M_{\text{Pl}}^2 \beta_{\text{kin}}^2 X_3 - U(\varphi_3), \quad U(\varphi_3) = 3M_{\text{Pl}}^2 H_I^2 \left(1 - e^{-\beta_1 \varphi_3} \right)^2, \quad (70)$$

where φ_3 is normalized to be dimensionless, α_{kick} , β_{kick} , β_{dip} , β_{kin} and β_{I} are all dimensionless parameters, and H_I is a constant of mass dimension 1. Note that setting $\varphi_3 = 0$ gives the case of the NEC-violating sector alone studied in the previous subsection.

The explicit but rather nontrivial forms of the interactions above are taken to accomplish the desired efficient energy transfer from the NEC-violating sector to reheat the Universe. One feature we aim for is to eventually yield to an oscillating reheating field φ_3 (as explained with fig. 5, and numerically verified in fig. 8). The above choices lead to the following dynamics:

- When the NEC is well preserved, φ_3 is effectively decoupled from φ_2 . Then, φ_3 stays at the minimum of its Starobinsky-type bare potential U , *i.e.* $\varphi_3 = 0$ while the NEC holds.
- During the time when the NEC violation takes place, the different potentials V and U together shape the reheating potential. The potential U gives the bare potential of φ_3 , while V generates an alternative local minimum for φ_3 (recall that v is negative) when φ_2 approaches to its origin. Thus φ_3 is moved to this new minimum at $\varphi_3 = 1$ during the NEC violation. This process is further discussed in section IV D.
- The overall factor introduced for F_1 and F_2 in eqs. (69) modulate the kinetic term of φ_2 , which takes 1 for $\varphi_3 = 0$ and the smaller value $(1 + \alpha_{\text{kick}})^{-1}$ for $\varphi_3 = 1$, while φ_3 is given an extra ‘kick’ through β_{kick} around the time of NEC violation.
- The function G_3 is taken independent of φ_3 and makes important contribution only during the NEC-violating phase. It returns to a negligible value afterwards, respecting the late-time constraints [28].

To summarize everything, our total action of eq. (20) consists of the functions K , G_3 and P , whose explicit forms are now

$$K = M_{\text{Pl}}^2 H_{\text{dip}}^2 \left[\frac{1 + \alpha_{\text{kick}} e^{-\beta_{\text{kick}} \varphi_3}}{1 + \alpha_{\text{kick}}} \left(F_1(\varphi_2) X_2 + F_2(\varphi_2) X_2^2 \right) - e^{-\beta_{\text{dip}}^2 ((\varphi_3 - 1)^2 - 1)} v(\varphi_2) \right], \quad (71a)$$

$$G_3 = M_{\text{Pl}}^2 H_{\text{necv}}(\varphi_2) F_{\text{kb}}(\varphi_2) X_2, \quad (71b)$$

$$P = M_{\text{Pl}}^2 \beta_{\text{kin}}^2 X_3 - U(\varphi_3), \quad (71c)$$

where v and F_{kb} are given by eq. (62), H_{necv} by eq. (63), F_1 and F_2 by eq. (64), and U by eq. (70). In the following subsection, we discuss the behavior of the effective potential for φ_3 in more detail.

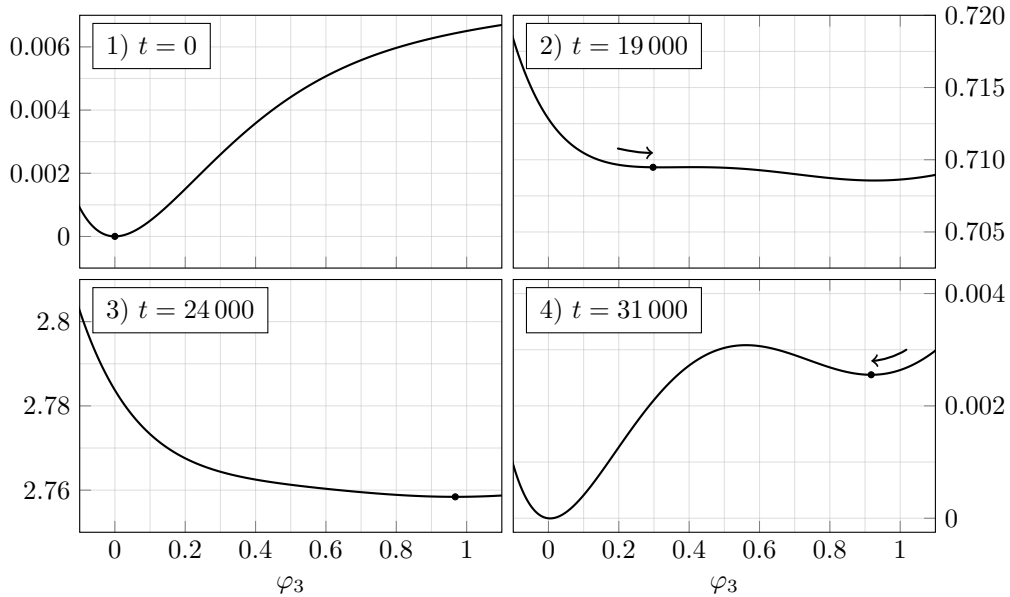


Figure 5. Evolution of φ_3 and the shape of its total effective potential, which is altered by φ_2 . (1) The field φ_3 starts here at zero, and (2) it is then raised, until it starts rolling down to (3) a new minimum. (4) As the potential regains its previous shape, the field φ_3 falls back into (1) its original position. We also call for attention to how the vertical scale changes.

D. The reheating potential

We have determined our full Lagrangian as in eqs. (20) and (71). The reconstruction procedure of section IV A is robust for the NEC-violating sector φ_2 as shown in section IV B, while the reintroduction of the reheating field φ_3 is done in section IV C in a rather *ad hoc* manner. In this subsection we further describe the trajectory that φ_3 is expected to take, which shall be verified numerically in section V. The reheating process operates essentially by the reheating field φ_3 rolling down to the minimum of its effective potential that is uplifted by the NEC violation. Then φ_3 starts oscillating, releasing its energy into the Universe. A coupling of φ_3 with the Standard Model particles is necessary, but implicit hereafter, and we do not specify its concrete form.

The time evolution of the effective potential of φ_3 is illustrated in fig. 5. The reheating procedure is essentially articulated around the evolution of φ_3 along its total potential whose shape is in turn driven by φ_2 in the following way. For most of the cosmic period in which the shift symmetry of φ_2 is well respected, the reheating field φ_3 stays at the minimum of its bare potential U . Once the NEC violation takes place by φ_2 , however, the reheating field φ_3 is transported upward and rolls to a new and higher minimum. Later toward the end of the NEC-violating phase, the interaction between φ_2 and φ_3 becomes ineffective, and φ_3 is subsequently sent back to the initial minimum.

On this return trajectory, the acquired kinetic energy results in oscillations around this minimum, leading to reheating of the Universe.

The shape of the bare potential $U(\varphi_3)$ is of the type of Starobinsky's inflation and is depicted in fig. 5 (1). The total, 'effective' potential for φ_3 consists not only of $U(\varphi_3)$ but of the contributions from $K(\varphi_2, X_2, \varphi_3)$, as is given in eq. (71a). A rough description of each term in K is as follows: while each term is approximately constant and takes a negligible value during the (long) NEC-preserving era, the term proportional to $F_1 X_2 + F_2 X_2^2$ is uplifted and erases the minimum around $\varphi_3 = 0$ during the NEC violation. The term proportional to v , on the other hand, arises and accommodates a new minimum at $\varphi_3 = 1$. The changing effective potential is visualized in fig. 5 (2) and (3). Toward the end of the NEC-violation period, the modulation by φ_2 effectively turns off, and φ_3 is drifted back to $\varphi_3 = 0$, as shown in fig. 5 (4).

The period during the NEC violation and before the reheating may as well accommodate inflation to produce the seeds of the structure formation. This is also an interesting possibility to realize, but is beyond the scope of our current work, and we leave it to future studies.

V. NUMERICAL APPROACH

Now that we have constructed all the ingredients to achieve the scenario of our interest, we proceed to its numerical verification in this section. Our goals are two-fold: to provide a concrete example in which our model can indeed violate the NEC in a stable manner, and to demonstrate that a successful reheating follows the NEC-violating period. We focus on the NEC-violating-reheating transitions in this work and do not include the cosmological constant relaxation sector φ_1 in our numerical computation, whose time scale is much longer than the former eras and would thus be computationally rather impractical. As far as the relaxation sector is concerned, we impose the condition of eq. (19) to ensure that the domination of φ_2 would not lead the motion of φ_1 to overshoot.

A. Implementation details

To execute the numerical integration of our model, we solve simultaneously the three equations of motion, *i.e.* eqs. (29b) to (29d). We use the constraint equation, eq. (29a), to monitor the numerical convergence, as it must be compatible with the time evolution of the system. The second derivatives enter the equations only linearly and are hence single-valued at a given time, and the

Function	H_{necv}	Function	F_{kb}	Function	v	Reheating φ_3 modulation		Reheating φ_3 sector	
H_0	10^{-3}	$F_{\text{kb},0}$	10^{-3}	v_0	$5 \cdot 10^{-2}$	α_{kick}	10^{-2}	β_{kin}	1
H_1	1	$F_{\text{kb},1}$	1	T_{dip}	$2T$	β_{kick}	5	β_I	3
T	5000	T_{kb}	$3T$	H_{dip}	$\frac{4H_1}{10} \sqrt{\frac{\alpha_{\text{kick}}}{1+\alpha_{\text{kick}}}}$	β_{dip}	2	H_I	$\frac{5H_1}{10} \sqrt{\frac{\alpha_{\text{kick}}}{1+\alpha_{\text{kick}}}}$
τ	500								

Table I. Compilation of all the numerical parameters used in the numerical computations.

system can be numerically solved using any standard integration algorithm.

The functions K , G_3 and P , appearing in the equations of motion, are substituted by eq. (71) together with v , F_{kb} , H_{necv} and U in eqs. (62a), (62b), (63) and (70), respectively, and F_1 and F_2 reconstructed as in eq. (64). In order to fix a reasonable set of model parameters, we choose the values compiled in table I for our numerical integration. The duration of the NEC-violating period relates to a few parameters, *i.e.* T , T_{kb} and T_{dip} , and we thus take them at roughly the same order of magnitude. The ending time of the NEC violation is controlled by τ , and since we demand the reheating field φ_3 transit back to its true potential minimum quickly enough to start oscillating, the value of τ is taken smaller than T . The parameter H_1 approximately normalizes the value of the Hubble expansion rate at the NEC-violating era, and we use it as the units for inverse time t^{-1} , amounting to fixing $H_1 = 1$. In seeking a solution of the approximate form $\partial_t \varphi_2 \sim 1$, we also measure φ_2 in the units of H_1^{-1} . In order for φ_2 to kinetically dominate the energy density during the NEC-violation, we take the values of H_{dip} and H_I smaller than H_1 . During the NEC violation the φ_2 field receives a small ‘kick’ associated with α_{kick} by the change of φ_3 . The value of H_0 is that of the Hubble expansion rate during the long-lasting NEC-preserving era, which is to our concern essentially the present Hubble value. It is thus supposed to be extremely small; however, such a huge hierarchy is rather difficult to handle in numerical computations, and we here take a relatively large (but much smaller than H_1) value $H_0 = 10^{-3}$ for the purpose of demonstration. Values of order unity are chosen for other parameters. The reduced Planck mass M_{Pl} does not affect the dynamics. Let us emphasize that this set of parameters are chosen to support a proof-of-concept, and other choices can show behaviors similar to the current study.

We take the initial time of the numerical integration well before the onset of the NEC violation. We choose to set the initial conditions as

$$\varphi_2 = -5T, \quad \dot{\varphi}_2 = 1, \quad \varphi_3 = 0, \quad \dot{\varphi}_3 = 0. \quad (72)$$

That is, the NEC-violation field φ_2 is assumed to be on its attractor solution, and our choice of φ_3

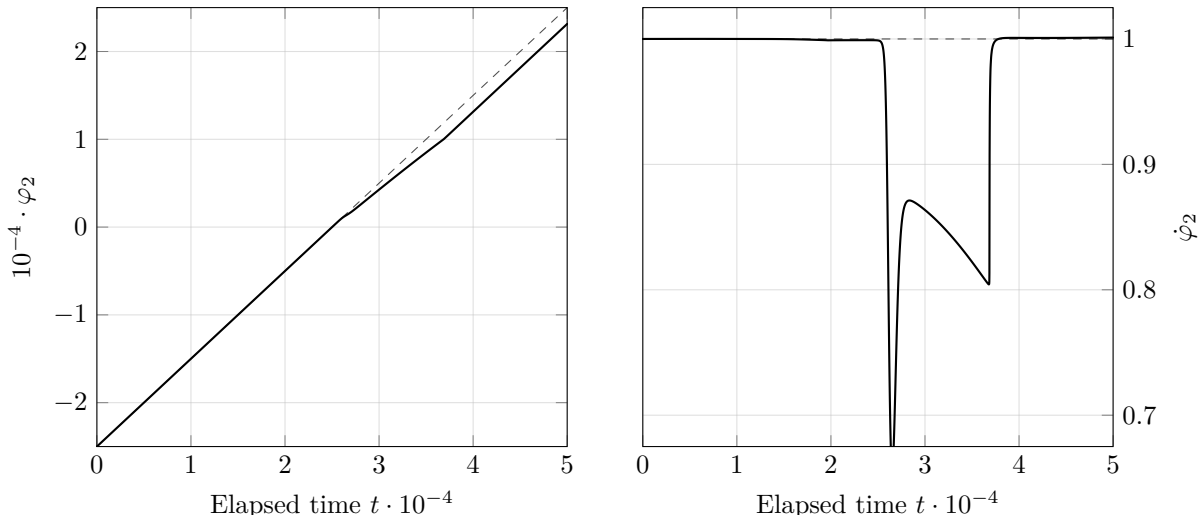


Figure 6. Time evolution of the NEC-violating field φ_2 on the left panel, and its time derivative $\dot{\varphi}_2$ on the right. The dashed line on the left corresponds to $\varphi_2 = t$, which would be the solution in the absence of φ_3 .

potential sets the minimum of φ_3 at the origin during the period of conserved NEC. Now all the ingredients are ready to perform the numerical computation.

B. Numerical results

We show the result plots in figs. 6 to 8. The first, fig. 6, depicts the trajectories for φ_2 and its time derivative $\dot{\varphi}_2$. As can be observed, the overall behavior is close to $\varphi_2 = t$, in accordance to the input eq. (61) of the reconstruction process, with a transient deviation during the NEC-violating phase. This indicates that φ_2 stays closely in the attractor regime discussed in section IV B, despite the additional ingredient for reheating, which is φ_3 . This justifies our separate treatment of the NEC-violation and reheating sectors in section IV and confirms the validity of our scenario.

The evolution of the Hubble expansion rate, shown in fig. 7, also verifies the desired behavior by violating the NEC violation for a finite duration. While the value of H drops toward the end of the NECV period around $t \approx 2.5 \cdot 10^4$, it does not reach its final value immediately, but instead it stays at a larger value for some time until finally dropping to the NEC-preserving value H_0 . This is due to the contribution from the reheating field φ_3 , which is trapped at the local minimum of its effective potential as illustrated in the bottom panels of fig. 5. Except for this small modulation, the overall behavior mimics the shape of the predetermined H_{necv} in eq. (63), which is co-drawn as a dashed curve in fig. 7.

Thanks to the NEC violation, φ_2 effectively stores energy, and the field φ_3 that is coupled to it

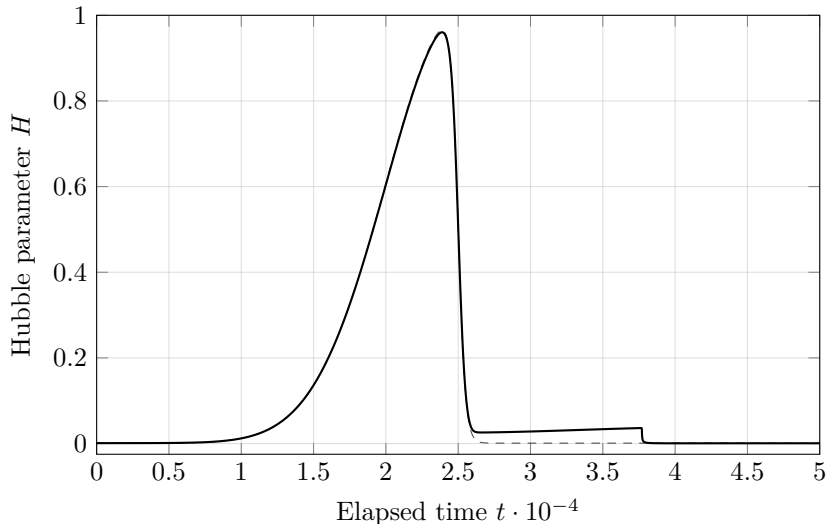


Figure 7. Time evolution of the Hubble expansion rate H . Notice the overall bell shape as well as the small drop at later times. The input shape H_{necv} (fig. 3) is here reminded by the dashed line, which would be the behavior of H in the absence of φ_3 .

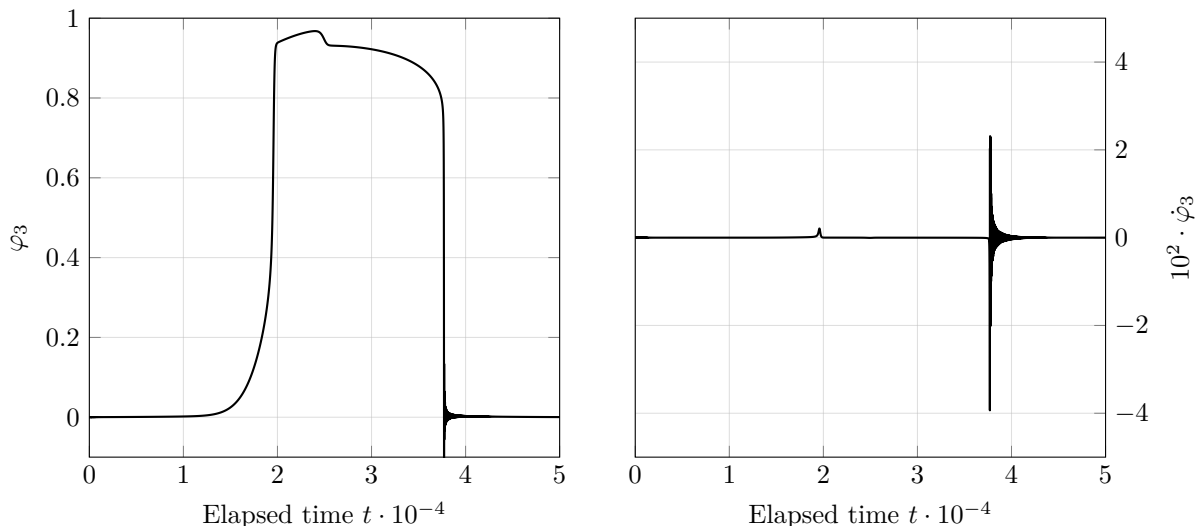


Figure 8. Time evolution of the reheating field φ_3 on the left, and its time derivative $\dot{\varphi}_3$ on the right. One can refer to fig. 5 to observe that φ_3 overall follows the target trajectory, and ends up oscillating on its return to the true minimum of the reheating potential. The latter oscillation is also clearly visible in the time derivative of φ_3 , as well as the comparatively small initial move to the temporary equilibrium position.

in turn acquires part of the energy to reheat the Universe. For successful reheating and efficient energy release, it is essential for φ_3 to actually rolls down at the end of NEC violation and start oscillating once it falls back to its true potential minimum. This is the dynamics indeed observed in the numerical evolution as in fig. 8. As seen, the initially stabilized φ_3 at $\varphi_3 = 0$ is displaced at

the beginning of the NEC-violating phase through its interaction with φ_2 . When H drops around $t \approx 2.5 \cdot 10^4$, φ_3 is left at the same local minimum, though its value slightly changes due to the drop. It stays there for some time, during which its effective potential regains the true minimum at the origin as illustrated in the bottom right panel of fig. 5. Eventually φ_3 drops toward the minimum and starts the oscillation, which is the moment reheating occurs. This concludes the concrete demonstration of the reheating mechanism of the Universe that would otherwise be empty after the relaxation phase of the cosmological constant.

A few consistency checks are in order. First, we ensure that the presence of the NEC violation should not mess up the relaxation mechanism, namely the condition for no overshooting, eq. (19), needs to be imposed. Under the current parametrization of the numerics, $\partial_t \varphi_2 \equiv M^2 \approx 1$, and t is measured in the units of H_1^{-1} , and so is φ_2 , where H_1 is approximately equal to the value of the Hubble expansion rate during the NEC violation. Then the condition of eq. (19) translates to

$$\frac{\Delta\varphi_2}{H_1^{-1}} \lesssim \left(\frac{M_{\text{Pl}}}{\sqrt{3} H_1} \right)^{4m-2} \frac{H_0^2}{M_{\text{Pl}}^2}. \quad (73)$$

In our example numerical computation, $\Delta\varphi_2$ for the NEC violation is about a few times 10^4 in the units of H_1^{-1} , and if we take $H_1 \sim 10^{12} \text{ GeV} \sim 10^{-6} M_{\text{Pl}}$, assuming a high NEC violating energy scale, we have $H_0 = 10^{-3} H_1 \sim 10^{-9} M_{\text{Pl}}$. Then the above condition of eq. (73) is satisfied for $m \gtrsim 1.45$, which is weaker than the theoretical constraint $m > 3/2$ already imposed (see after eq. (10)). Note that the realistic value of H_0 is much smaller than that taken in our numerical example, and nonetheless the condition can be met for a larger value of m without difficulty.

Moreover, we can easily verify that the stability conditions against small perturbations are also fulfilled in our result. Among the no-ghost conditions summarized in eq. (51), the second one, $\mathcal{G}_\varphi > 0$, is trivially satisfied with our choice $P \propto X_3$ (*i.e.* $\mathcal{G}_\varphi = M_{\text{Pl}}^2 \beta_{\text{kin}}^2$), and the first one, $\mathcal{G}_S > 0$, is numerically confirmed in fig. 9. On the other hand, the squared sound speeds c_s^2 obtained in eq. (58) do not invoke any instabilities. One of the values is trivially unity, $c_\chi^2 = 1$, in our case, and the other, $c_s^2 = \mathcal{F}_S/\mathcal{G}_S + \mathcal{A}$, is shown to be bounded by $0 < c_s^2 < 1$ in fig. 10 for the entire duration of the computation, and thus neither gradient instability nor superluminality is present.

The above results therefore show the realization of our target scenario: while φ_1 operates the relaxation mechanism of cosmological constant, reviewed in section II A, the field φ_2 stably violates the NEC, and the reheating field φ_3 moves to a new minimum, before oscillating on its way back to its true minimum and eventually reheating the Universe.

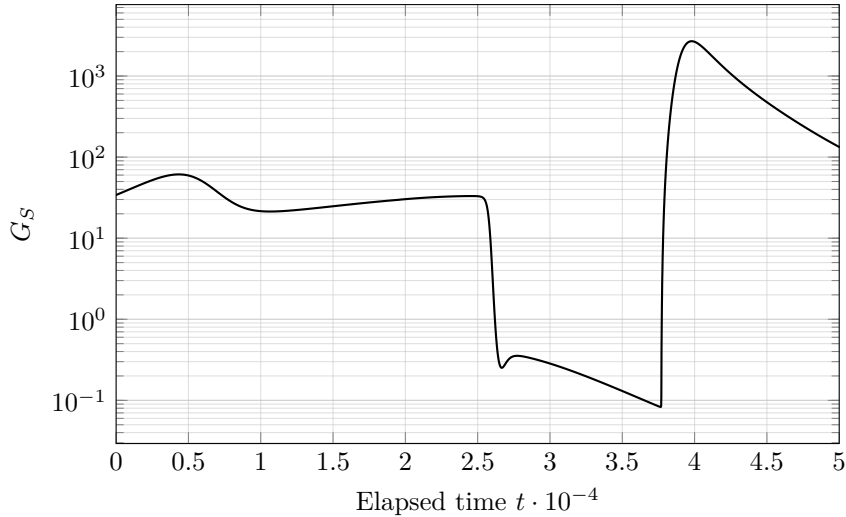


Figure 9. Time evolution of the no-ghost condition \mathcal{G}_S , defined in eq. (50). Its value is observed to remain positive, satisfying the first no-ghost condition in eq. (51). Note that the other no-ghost condition is trivially satisfied, see the main text.

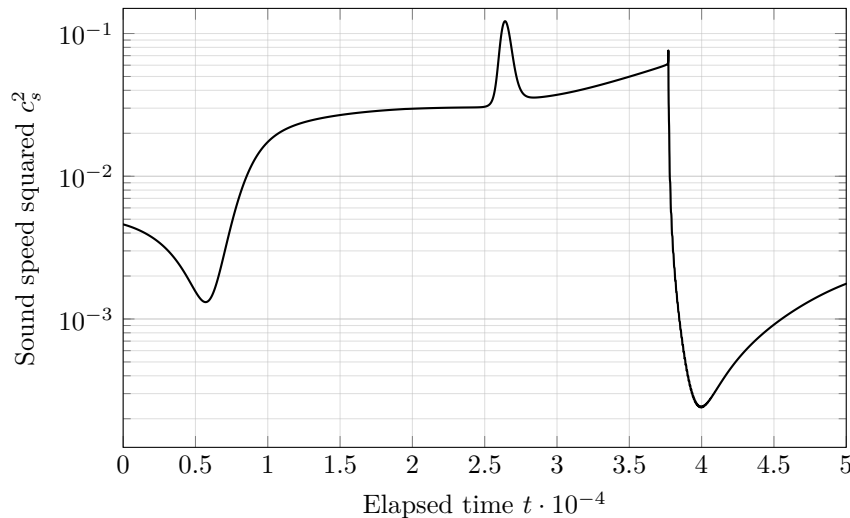


Figure 10. The square of the speed of sound, c_s^2 , remains strictly positive and below unity during the whole cosmic history, showing the absence of gradient instability and superluminality. The other sound speed is trivially 1 in our present case.

VI. CONCLUSION AND OUTLOOK

The current work exhibits a concrete model that both answers to the cosmological constant problem by dynamically relaxing the c.c., and subsequently reheats the Universe (section II). It builds upon two previous works, [1, 2] and [23], and extends the studies on stability and potential

overshooting issues with numerical confirmation. This work provides a conceptual proof of a system that resolves the c.c. problem without fine-tuning.

Our proposed model is the stable assembly of three components. Firstly, the model introduces a scalar field φ_1 [1, 2] equipped with an atypical kinetic term modulated by an inverse power of the spacetime curvature invariant, which effectively lets the field φ_1 roll down and eventually has its potential converge to a tiny, but positive value. This final value becomes an effective c.c.. This dynamical relaxation process ‘feels’ the value of any existing contributions to the c.c., including quantum vacuum energy, and fixes the classical vacuum expectation value of φ_1 such that it cancels out the c.c.. The mechanism is not vulnerable to radiative corrections to curvature either, thus enjoying the advantage of avoiding known fine-tuning issues associated with c.c.. However, it also effectively empties the Universe, by diluting its contents such as radiation and matter by the cosmic expansion. This is by construction an inevitable consequence from the φ_1 sector alone, and an additional ingredient is in need for successful cosmology.

Secondly, to resolve this newly introduced issue, two other scalar fields φ_2 and φ_3 work together to violate the null-energy condition and repopulate our Universe. The former field φ_2 goes through the dynamics that effectively raises the value of the Hubble expansion rate for transient periods, thus breaking the null-energy condition. In order to ensure that the NEC violation does not destroy the c.c. relaxation mechanism of φ_1 , we impose the condition of eq. (19) to avoid the case in which φ_2 ’s motion irreversibly lets φ_1 overshoot the zero of the effective c.c.. We also require the time scale of the former be much shorter than that of the latter, giving sufficient time for the c.c. relaxation to operate, and that φ_2 respects (approximate) shift symmetry in the regions where the NEC is preserved. Moreover, for the sake of naturalness with respect to the timing of NEC violation, the field space of φ_2 is assumed to be periodic with a period much longer than the duration of a single NEC violation phase. This way our Universe goes through this phase multiple times and our current Universe merely occurs after many cycles of them. The field φ_3 acts as a reheating field that extracts the energy from the NEC violation sector, starts oscillating after it, and eventually reheats the Universe.

Thirdly, the last component of our model is the gravity sector. It has non-minimal couplings to φ_1 and φ_2 , as already described. As the metric-only part, together with the standard Einstein-Hilbert term, our action includes the quadratic term of the Ricci scalar, which stabilizes the c.c. relaxation sector [1, 2]. These three ingredients together achieve our complete cosmological scenario of c.c. relaxation, NEC violation, and reheating, in a stable manner.

In order to concretely realize the desired cosmological history, the model functions need to be

fixed, and we proceed to their reconstruction in section IV. While we determine the φ_2 sector in an unambiguous manner, the way φ_3 is included is rather *ad hoc*. Nevertheless we conduct numerical integration for the entire system of φ_2 and φ_3 (but without φ_1 , for numerical ease) in section V, thus justifying our methodology and confirming the realization of NEC violation followed by a reheating phase. The stability conditions against small perturbations are also shown to be respected.

In our numerical example, the energy used for reheating is roughly one order of magnitude smaller than the energy acquired by the NEC violation in the units of H , as seen in figs. 7 and 8. This is basically the limitation due of the concrete implementation we have chosen, and we leave to future studies the possibility of more efficient energy transfer and higher reheating scale. Moreover, our current choice of parameters does not accommodate an inflationary phase and thus has no implications (for now) for the structure formation and cosmic microwave background anisotropies. The connection to these observables is beyond the scope of our present work, as satisfying all the stability conditions simultaneously is already a non-trivial task in the minimal scenario. We would like to return to this issue in the future work.

Our model is based on the Horndeski class of theories to violate the NEC. As an another possibility, the so-called minimally modified gravity theories [29–31] could be an interesting candidate. While this class of theory contains only two degrees of freedom and consequently avoids instabilities with no difficulty, it nonetheless allows a large freedom for background evolution, not limited by energy conditions. Our conceptual scenario may thus provide a fertile ground for model buildings.

The concrete model considered in this work is an effective theory. Linking it to some more fundamental UV theory could also lead to an interesting path to explore. That would accomplish a complete, self-containing solution to the long-standing c.c. problem. We wish our present study gives one step forward in healing this conceptual pathology.

-
- [1] Shinji Mukohyama and Lisa Randall. A Dynamical approach to the cosmological constant. *Physical Review Letters*, 92:211302, 2004.
 - [2] Shinji Mukohyama. Gravity in the dynamical approach to the cosmological constant. *Physical Review D*, 70:063505, 2004.
 - [3] Adam G. Riess, Lucas Macri, Stefano Casertano, Hubert Lampeitl, Henry C. Ferguson, Alexei V. Filippenko, Saurabh W. Jha, Weidong Li, and Ryan Chornock. A 3space telescope and wide field camera 3. *The Astrophysical Journal*, 730(2):119, Mar 2011.
 - [4] N. Aghanim et al. Planck 2018 results. VI. Cosmological parameters. *Astron. Astrophys.*, 641:A6, 2020.

- [Erratum: Astron.Astrophys. 652, C4 (2021)].
- [5] V. Bonvin et al. H0LiCOW – V. New COSMOGRAIL time delays of HE 0435–1223: H_0 to 3.8 per cent precision from strong lensing in a flat Λ CDM model. *Mon. Not. Roy. Astron. Soc.*, 465(4):4914–4930, 2017.
 - [6] Jose Luis Bernal, Licia Verde, and Adam G. Riess. The trouble with H_0 . *JCAP*, 10:019, 2016.
 - [7] Adam G. Riess et al. A Comprehensive Measurement of the Local Value of the Hubble Constant with 1 km/s/Mpc Uncertainty from the Hubble Space Telescope and the SH0ES Team. 12 2021.
 - [8] Steven Weinberg. The Cosmological Constant Problem. *Rev. Mod. Phys.*, 61:1–23, 1989.
 - [9] Jerome Martin. Everything You Always Wanted To Know About The Cosmological Constant Problem (But Were Afraid To Ask). *Comptes Rendus Physique*, 13:566–665, 2012.
 - [10] Antonio Padilla. Lectures on the Cosmological Constant Problem. 2 2015.
 - [11] H. E. S. Velten, R. F. vom Marttens, and W. Zimdahl. Aspects of the cosmological “coincidence problem”. *Eur. Phys. J. C*, 74(11):3160, 2014.
 - [12] V. A. Rubakov. Relaxation of the cosmological constant at inflation? *Phys. Rev. D*, 61:061501, 2000.
 - [13] Peter W. Graham, David E. Kaplan, and Surjeet Rajendran. Relaxation of the cosmological constant. *Physical Review D*, 100(1):015048, 2019.
 - [14] Nima Arkani-Hamed, Savas Dimopoulos, Nemanja Kaloper, and Raman Sundrum. A Small cosmological constant from a large extra dimension. *Phys. Lett. B*, 480:193–199, 2000.
 - [15] Osmin Lacombe and Shinji Mukohyama. Self-tuning of the cosmological constant in brane-worlds with $P(X, \phi)$. 3 2022.
 - [16] Oleg Evnin, Victor Massart, and Kévin Nguyen. Robustness of the cosmological constant damping mechanism through matter eras. October 2020.
 - [17] Ichiro Oda. Scale Symmetry and Weinberg’s No-go Theorem in the Cosmological Constant Problem. *Adv. Stud. Theor. Phys.*, 13:195–214, 2019.
 - [18] Tsutomu Kobayashi, Masahide Yamaguchi, and Jun’ichi Yokoyama. Generalized G-inflation: Inflation with the most general second-order field equations. *Progress of Theoretical Physics*, 126:511–529, 2011.
 - [19] Gregory Walter Horndeski. Second-order scalar-tensor field equations in a four-dimensional space. *Int. J. Theor. Phys.*, 10:363–384, 1974.
 - [20] C. Deffayet, Xian Gao, D. A. Steer, and G. Zahariade. From k-essence to generalised galileons. *Physical Review D: Particles and Fields*, 84:064039, 2011.
 - [21] V. A. Rubakov. The null energy condition and its violation. *Physics-Uspekhi*, 57:128–142, 2014.
 - [22] Sakine Nishi and Tsutomu Kobayashi. Reheating and primordial gravitational waves in generalized galilean genesis. *JCAP*, 04:018, 2016.
 - [23] Lasma Alberte, Paolo Creminelli, Andrei Khmelnitsky, David Pirtskhalava, and Enrico Trincherini. Relaxing the cosmological constant: A proof of concept. *JHEP*, 12:022, 2016.
 - [24] Antonio De Felice, Shinji Mukohyama, and Shinji Tsujikawa. Density perturbations in general modified gravitational theories. *Phys. Rev. D*, 82:023524, 2010.

- [25] Nima Arkani-Hamed, Hsin-Chia Cheng, Markus A. Luty, and Shinji Mukohyama. Ghost condensation and a consistent infrared modification of gravity. *JHEP*, 05:074, 2004.
- [26] Nima Arkani-Hamed, Paolo Creminelli, Shinji Mukohyama, and Matias Zaldarriaga. Ghost inflation. *JCAP*, 04:001, 2004.
- [27] Tsutomu Kobayashi, Norihiro Tanahashi, and Masahide Yamaguchi. Multifield extension of G inflation. *Phys. Rev. D*, 88(8):083504, 2013.
- [28] Paolo Creminelli, Giovanni Tambalo, Filippo Vernizzi, and Vicharit Yingcharoenrat. Dark-Energy Instabilities induced by Gravitational Waves. *JCAP*, 05:002, 2020.
- [29] Chunshan Lin and Shinji Mukohyama. A Class of Minimally Modified Gravity Theories. *JCAP*, 10:033, 2017.
- [30] Shinji Mukohyama and Karim Noui. Minimally Modified Gravity: a Hamiltonian Construction. *JCAP*, 07:049, 2019.
- [31] Antonio De Felice, Andreas Doll, and Shinji Mukohyama. A theory of type-II minimally modified gravity. *JCAP*, 09:034, 2020.